A

Major Project thesis

On

"The Analysis of Casting Design for Junction Considering Solidification"

Submitted in partial fulfillment for the requirement of the degree of

Masters of Engineering

in

Production and Industrial Engineering

By

JITENDRA KUMAR PANDEY

Roll No.: 8602(2004-2006)

Under the guidance of

PROF. A.K. MADAN

DEPARTMENT OF MECHANICAL ENGINEERING

DELHI COLLEGE OF ENGINEERING

DELHI UNIVERSITY, DELHI-42

Department of Mechanical Engineering
Delhi College of Engineering, Delhi-42

CERTIFICATE

This is to certify that the project entitled **"The Analysis of Casting Design for Junction Considering Solidification"**, which is being submitted by Jitendra Kumar Pandey of student's own work carried by him under my guidance and supervision in partial fulfillment of requirement for the award of the Degree of **Master of Engineering in Production Engineering, Department of Mechanical Engineering, Delhi College of Engineering, University of Delhi.**

The matter embodied in this project has not been submitted for the award

Dr. S Maji
Prof & Head
Department of Mechanical Engg.
Delhi college of Delhi, Delhi

Mr. A.K.Madan
Lecturer
Department of Mechanical Engg.
Delhi college of Delhi, Delhi

Acknowledgment

The beauty of the Destination is half veiled and the fragrance of success half dull, until the traces of these enlightening the path are left to fly with the wind spreading the words of thankfulness .'

Here, I wish to express my heartily and sincere gratitude and indebtedness to Mr.A.K.Madan Professor of Mechanical Engineering Department, Delhi College of Engineering, Delhi for his valuable guidance and wholehearted cooperation. He has a special place in my heart for many reasons but to be limited, he is the one who generated confidence in my inner being and helped my hidden energies to come out in full. I like to thank my seniors specially Mr. P.Ghosh (SR.Mgr.Production, HAL) and my collogues who helped me a lot during my project completion. I am also thankful to my team members for help me in supplying valuable information and data.

My heartily thanks to all my professors for their expertise and all rounded personality they have imparted me.

My credit also goes to all my pals for their humor, innocence, too much sincerity and cooperation, openness and the like which flourishes my stay here.

Finally, I have shortage of words to express my love and thanks to my beloved parents to whom I know my knowledge

JITENDRA KUMAR PANDEY

CONTENTS

LIST OF FIGURES

LIST OF TABLES

Nomenclature

T	Temperature (k)
H	Enthalpy
P	Density (kg/m3)
K	Coefficient of thermal conductivity
τ	Time (sec)
q	Heat flux (w/m2)
c	Specific heat (J/kg-k)
N	Shape function
n	Normal to surface
σ	Boltzmann's constant (w/m2-k4)
ε	Emissivity
F	Form factor
L	Latent heat (j/kg)
V	Volume (m3)
A	Area (m2)

Abstract

Casting junctions, intersections of two or more sections leading to mass concentration, are potential location of shrinkage cavity or porosity. The shrinkage defects can be predicted by physics based numerical simulation. Two mathematical models are available: (a) critical solid fraction loop based upon temperature profile and (b) Niyama criteria, which is based on thermal gradient. By using finite element (FE) methods, it is possible to solve the transient heat transfer problem and predict the location, extent of shrinkage cavity and porosity.

This project aims at carrying out FE analysis of standard junctions such as L, V, and T followed by the comparison of results with experimental observation available in literature for steel. The Niyama criterion was found to be superior to the critical solid fraction loop approach.

Further, the results of simulation are input to regression analysis to evolve a set of empirical equations to quickly predict shrinkage porosity in different types of junctions. These equations are expected to be very useful for design for manufacture of casting beforefreezing there design.

Keywords: Casting junctions, Finite element method, Design guidelines, Shrinkage cavity

Chapter 1

Introduction

1.1 Casting Process

Casting process gives the shortest routes from raw material to finished part (Dieter, 983). In this process, molten metal is poured into a mould or cavity that is similar to the shape ofthe finished part. It is very complex owing to the following:

1. Solidification of pure metals proceeds layer-by-layer starting from the mould wall and moves inward. As metal solidifies, it contracts in volume and draws molten metal from adjacent (inner) liquid layer. So at hot spot, there is no liquid metal left and a void called shrinkage cavity is formed.

2. Alloys solidify over a range of a temperature. Freezing rate affects the casting Microstructures, mainly the grain size.

3. Feeders are designed to compensate the solidification shrinkage of a casting, so that it is free of shrinkage porosity. Feeder design parameters include the number, location, shape, and dimensions of feeders. It is cut off after casting solidification.

4. Temperature history of a location inside the casting with respect to neighboring Location governs the formation of shrinkage cavity. It is difficult to get temperature Histories since all modes of heat transfer are involved.

5. The rate of heat transfer from casting to the mould is affectedly the interface heat Transfer coefficient. It depends on the thickness of oxide layer and the air gap at the Interface. The air gap depends on the amount of gas generated.

6. The flow of molten metal after being poured is a transient phenomenon accompanied by turbulence, splashing, separation of streams near change of sections, branching off and rejoining of streams, and the onset of solidification. These affect the quality of casting.

1.2 Defects

In casting there are many types of defects like blow holes, pinholes, porosity, drop, inclusion, dross, dirt, misrun, cold shut, hot tear, shrinkage cavity, and shifts. Of these, shrinkage is one of the most important defects, especially in junctions, which is the focus of this work.

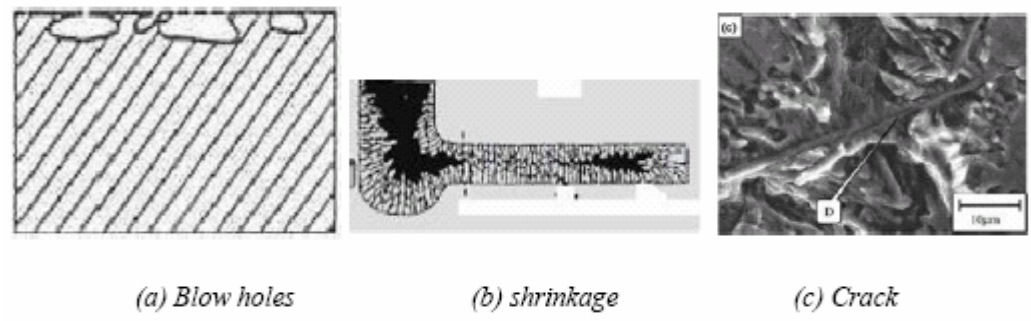

Figure 1.1: Some defects in casting (Gao, et al., 2004)

There are three distinct stages of shrinkage as molten metals solidify: liquid shrinkage, liquid to solid shrinkage and patternmaker's contraction (Gwyn, 1987).

• **Liquid shrinkage:** It is the contraction of liquid before solidification begins.

• **Liquid to solid shrinkage:** It is the shrinkage of metal mass as it transforms from the liquid's disconnected atoms and molecules into the saturated building blocks of solid metal. The amount of solidification shrinkage varies greatly from alloy to alloy.

• **Patternmaker's contraction:** It is the contraction that occurs after the metal has completely solidified to ambient temperature. Contraction is dictated by the alloy's rate of contraction. Shrinkage defects can be broadly classified based on size, as macro shrinkage and micro shrinkage (Ravi, 2005).

Macro shrinkage: This appears as a concentrated zone of shrinkage holes or even a single shrinkage cavity with irregular shape and rough surface. It occurs at isolated hot spots in short freezing range alloys. Typical locations are middle of thick sections, junctions, corners and region between two or more cores. A special form of macro shrinkage is the shrinkage pipe, which occurs in upper portion of a feeder in short freezing range alloy, typical locations are middle of thick sections, junctions, corners and

region between two or more cores. A special form of macro shrinkage is the shrinkage pipe, which occurs in upper portion of a feeder in short freezing range alloy, taking the shape of inverted cone.

Micro shrinkage: It appears like porosity or small holes of rough surface and usually detected during machining. It invariably occurs in castings of long freezing range alloys. It may be barely visible to naked eye.

1.3 Influencing Factors

The influencing factors of casting are categorized into three major categories based on process, material, and geometric complexity.

Slag/ dross formation tendency: Slag typically refers to high temperature fluxing of Refractory linings of furnaces /ladles and oxidation products from alloying. Dross typically refers to oxidation or reoxidation products in liquid metal from reaction with air during melting or pouring, and can be associated with either high or low pouring temperature alloys. Good melting, ladling, pouring and gating practice can avoid it. Ceramic filters are also used to avoid this.

Pouring temperature: Even though moulds must withstand extremely high temperatures of liquid metals, interestingly, there are not many choices of materials with refractory characteristics. When pouring temperature approaches a mould material refractory limit, the heat transfer patterns of the casting geometry become important. Sand and ceramic materials with refractory limits of 3000-3300°F (1650-1820°C) are the most common mould materials. Metal moulds, such as those used in die-casting and permanent moulding, have temperature limitations. Except for special thin designs, all alloys that have pouring temperatures above 2150°F (1180°C) are beyond the refractory capability of metal moulds.

Fluidity: It indicates the ability of metal to flow through a given mould passage. It is Quantified in terms of the solidified length of a standard spiral casting. The casting fluidity is driven by metallostatic pressure and hindered by viscosity and surface tension of molten metal, heat diffusivity of mould, back pressure of air in mould cavity and friction between the metal-mould pair.

Solidification shrinkage: As metal solidifies, it contracts in volume and draws molten metal from adjacent (inner) liquid layer. So at hot spot, there is no liquid metal left and a void called shrinkage cavity is formed. It varies from material to material.

External and internal shape: Part geometry directly affects complexity. The location of parting line depends on the extent of undercuts, which in turn depends on internal features in the part. A non-planer parting line must be avoided. This implies designing the product considering a perpendicular draw direction, minimizing undercuts and tapering the sections parallel to the draw direction to provide natural draft.

Types of cores: Cores enable internal features (through holes, undercuts, and intricate or special surface) to be produced in a cast product. Cores may also lead to defects related to mould filling (blow holes) and casting solidification (hot spots). The product designer must minimize the number of holes and reduce their complexity to the extent possible. The criteria related to cored holes include its minimum diameter, aspect ratio, location in thick section, distance from edge and distance from neighboring hole.

Minimum wall thickness: Fluidity of metal decides the minimum wall thickness. If fluidity is not enough then molten metal does not completely fill a section of the mould cavity. In this case, molten metal solidify before complete filling of mould.

1.4 Casting Design

Design of a component as casting requires close co-ordination between mechanical engineer making a functional design from various stress calculations and foundry engineer to modify the design to suit foundry process of manufacture for optimal performance and cost (Chen, et al., 1997). Good knowledge of capabilities of the casting process in terms of strength, characteristics of the cast metal, dimensional tolerances, surface finish, maximum wall thickness possible and the effect of quality on cost per piece will be of immense help to the designer. A specialist foundry engineer can also help in design changes for reduction of production problems in modeling, core making reduce production costs and improve quality.

Main casting design parameters are as follows:

(a) Selection of casting alloy.

(b) Casting process parameters

(c) Casting geometry consideration.

(d) Reducing casting process cost.

The Main problem in design of junction is shrinkage defect. In general, metal in Casting solidifies from the mould surface toward the center of the section. Thin sections will freeze before heavy sections. When the only source of feed metal for a heavy section is through a thin section, the thin section can freeze first and shut off the source of feed metal for heavy section. With no source of feed metal to replace the volume lost because of metal shrinkage, a heavy section will become porous. Also, with the onset of freezing, the thinner section starts to contract while the heavy section is still solidifying. This can cause stress to develop in the casting, resulting in cracks at hottest (weakest) section. Design for manufacturability (DFM) helps in casting design.

1.5 Design for Manufacturability (DFM)

Designing a product to be produced in the most efficient manner possible in terms of time, money, and resources, taking into consideration how the product will be processed, Utilizing the existing skill (and avoiding the learning curve) to achieve the highest yields Possible is referred to as DFM.

Characteristics: Some characteristics related to DFM are listed below.

- Focus on obtaining high quality and economy by design.
- Early prediction and prevention of production problems.
- Concurrent design of product and process.
- Product specs are compatible with process capability.
- Minimize negative environmental impact of the product.
- Reduce cost of complexity.

The DFM techniques should strike a balance between the information available at the Design stage and the information generated regarding manufacturability. For wider Acceptability, they should require only the essential features of a casting and be fast and easy to use. One technique, which relies on the features information of a casting, is "estimation of tooling and processing cost" (Ravi, 1998). In this approach, the presence and attributes of features are used for estimating the relative costs of tooling and manufacturing for different design alternatives. This initially requires collection and

analysis of extensive cost data from industry for a particular process. In this system, the part is assigned a multi digit code based on features such as undercuts, parting, cavity detail, ribs and bosses, surface finish and inserts. Based on this code cost estimates are obtained using a look-up table and are used for comparing design alternatives.

1.6 Report Organization

This report is organized in the following manner.

Chapter 1 gives introduction of casting process, defects of casting, and casting design.

Chapter 2 gives detail literature review regarding junction design guidelines, solidification phenomenon and solving techniques.

Chapter 3 introduces the problem in detail.

Chapter 4 gives information about shrinkage predication method and their application on junction.

Chapter 5 discusses the results in detail.

Chapter 6 includes the conclusions and future work.

Chapter 2

Literature Review

2.1 Casting Junction

A junction is a region in which different section shapes come together within an overall casting geometry (Gwyn, 1987). Simply stated, junctions are the intersection of two or more casting sections.

2.1.1 Junction types and parameters

There are five types of junction represented by L, V, T, Y, and X. All other configurations at corners could be considered as modification of one or more of these five. Comparisons of design for a particular junction are discussed in the next section (ASM, 1962). The parameters of a junction include the number of meeting sections, their thicknesses (absolute and relative), angle between them and fillet radius. For example, in a T-junction caused by a rib, the rib thickness must be about half of the connected wall thickness, and the fillet radius must be about 0.3 times the wall thickness. In L-junction, the fillet at inner corner must be about 0.5 times the wall thickness. In general, mass concentration, coupled with multiple junctions, especially at sharp angles, should be avoided. Fillets are used at junctions to eliminate sharp inside corners and the attendant problems of stress concentration. In practice, the stress developed in the casting during solidification and cooling is more important in determining fillet size than is wall thickness of the casting. For example, the fillet radii required in a casting of the I-beam are larger than those required in Tsection. In cooling of the I-beam type of casting, stresses are set up because the contraction of the web section is restrained by mould material between the standing flanges of the I section as shown in figure 2.1(a). Thus a larger fillet at junctions of I-section is required, to prevent hot tearing at the fillet area. In the T-section, because the casting is free to contract as shown in figure 2.1(b), the mould material sets up no cooling stresses and hence smaller fillets are practical.

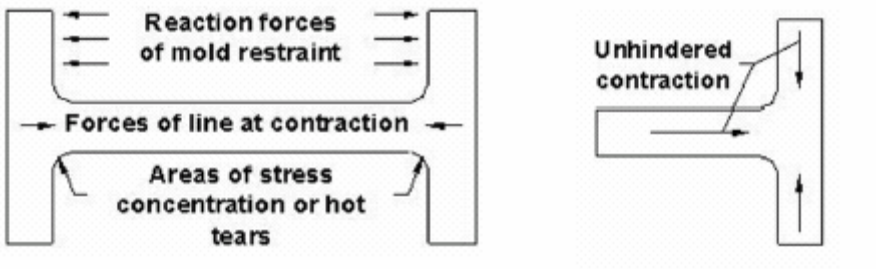

Figure 2.1: Residual stress

When fillets are required in an area where the junctions can serve as flow and feed paths for molten metal, it is advantageous to taper the fillets so that largest area lies nearest to riser and smallest area lies away from it. Figure 2.2 illustrates tapering fillets from a riser to the extremities of a casting which encourages soundness and often permits reduction in the weight of casting.

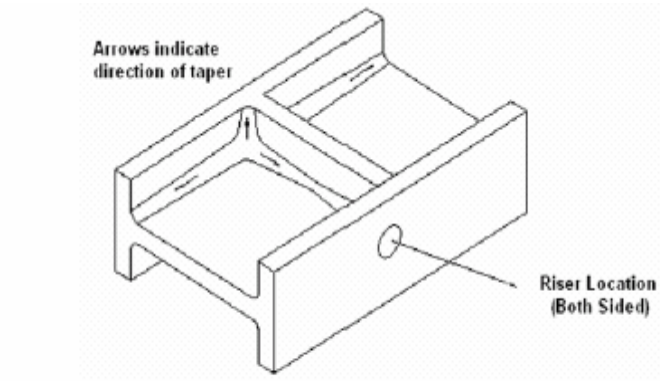

Figure 2.2: Tapering fillets from a riser to the extremities of casting

This tapering helps in freezing. Because of the tapering of the fillet in the junction, freezing

will progress toward the riser; this assures adequate feeding of junctions by the riser.

2.1.2 Junction design guidelines

The design guidelines are applicable for both equal and unequal cross-sectioned junction and described here.

Equal sections: This discussion gives information about iron casting. The following data is taken from casting design hand book. The cross-section of the castings that were used was 3 X 3 inches and the length of the arms was 24 inches with risers placed at extreme ends. The risers were utilized as sprue for pouring. Three inch sections were chosen because they were large enough to exhibit pronounced defects and were less sensitive to variations in the mould and metal temperature than thinner sections.

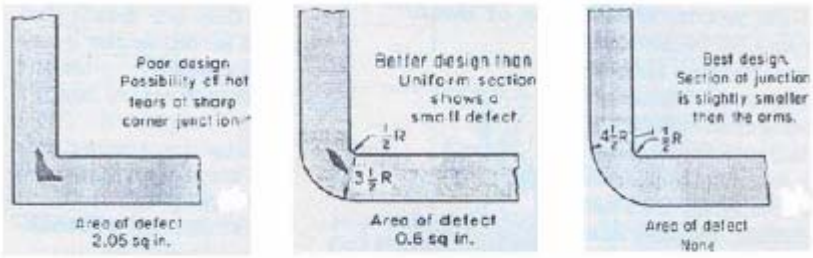

(a) Defect=2.05 sq. In. (b) Defect =0.6 sq. In. (c) No defect

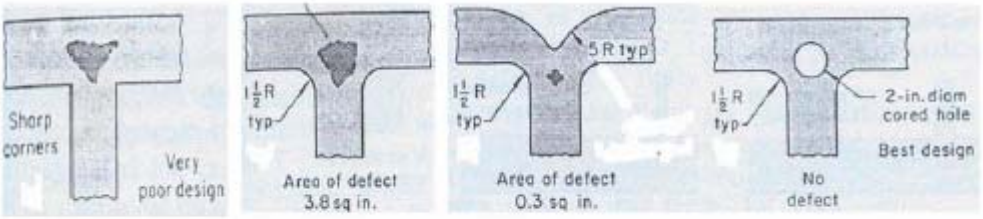

(d) Defect =3.5 sq. in (e) Defect =3.8 sq. in (f) Defect =0.3 sq. in (g) No defect

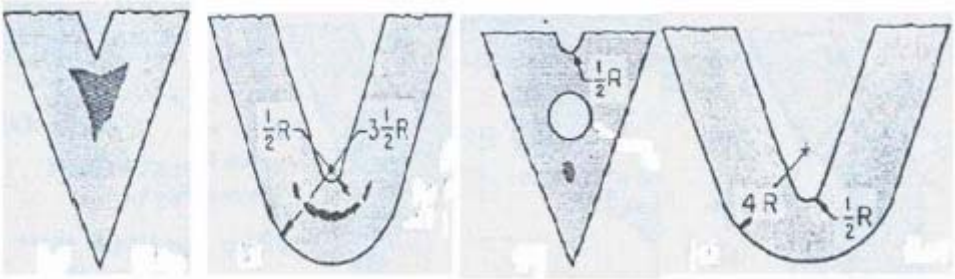

(h) Defect =3.3sq.in. (i) Defect =0.3sq.in (j) Defect =0.3 sq. in. (k) No defect

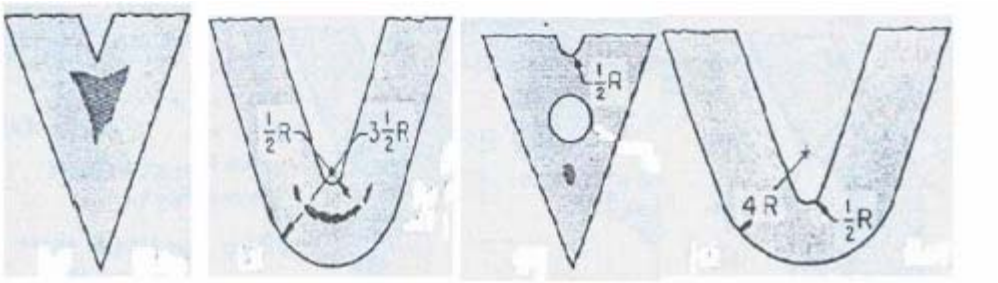

(h) Defect =3.3sq.in. (i) Defect =0.3sq.in (j) Defect =0.3 sq. in. (k) No defect

Figure 2.3: Comparison of defects in L.T, and V-sections (ASM, 1962)

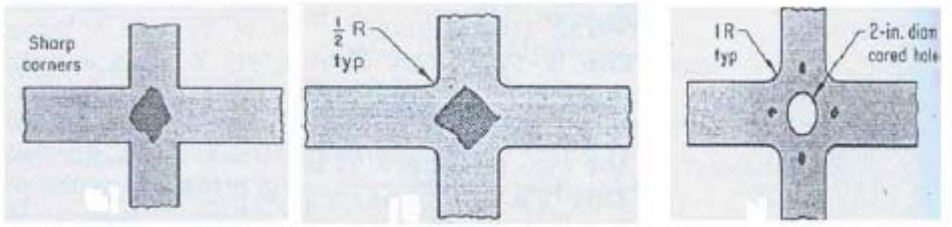

(a) Defect =5.5sq. in (b) Defect =6.4 sq. in (c) Very small cavity

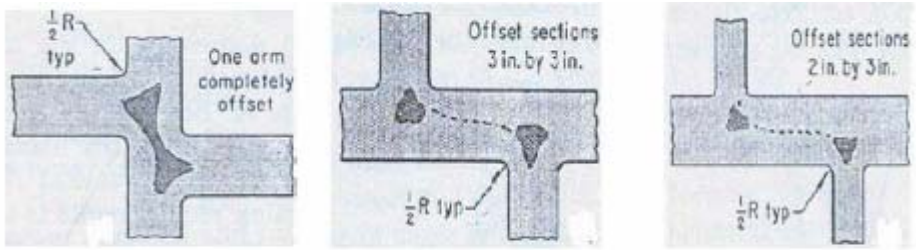

(d) Defect =5.5 sq. in (e) Total Defect = 4.3 sq. in. (f) Defect = 2.0 sq in.

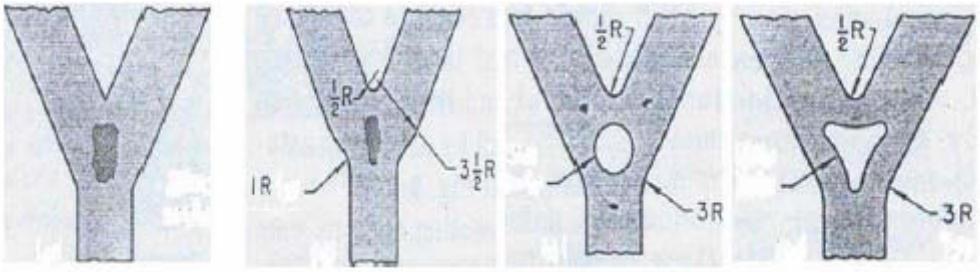

(g) Defect =2.7sq.in (h) Defect =2sq.in (i) Less defect (j) No defect

Figure 2.4: Comparison of defect in X and Y junction (ASM, 1962)

The castings were examined radiographically in a manner that reproduced the defects full size on x-ray film.

In **L-junction,** defects can be eliminated by using a ½ inch fillet and reducing the Wall thickness at the corner. When radius of the fillet is equal to wall thickness, there is no defect. There may be a centerline weakness when two freezing fronts meet each other (Figure 2.3).

Defects can be eliminated by making a hole in **T- junction**. A depression in the Cross arm of T-junction substantially reduces the defect but does not eliminate it.

When **V-junction** is formed by uniform sections then it will not be free from Shrinkage cavities, primarily because a hot spot is readily developed in the mold at the junction between the two sections. Mould sand which is a poor conductor of heat, cannot conduct the heat away from the sand enclosed between the sections of casting as quickly as the heat is transferred from molten metal into this mould section due to which mould becomes too hot. As a result the molten metal of that part freezes last. The defect decreases in area as the inside radius at the V- junction increases in size.

Coring a hole through the junction reduces porosity defect in **X-junction**. Sometimes this may not be practical. Defects can also be reduced by offsetting the section (Figure 2.4).

Defects can be eliminated in **Y-junction** by a triangular hole. Round hole can Decrease the defect but will be unable to eliminate it completely. If the riser is located on the junction then the defect is less.

However whenever the feeding of the molten metal at the junctions is inadequate During cooling and solidification, shrinkage defects would occur.

Unequal sections: When walls of two different thicknesses form a junction, it is advisable to incorporate a gradual increase in thickness of thinner section so that it is about equal in thickness with the heavier section at the point of juncture. Sharp corner, however is likely to contain larger shrinkage defects than those present with the round

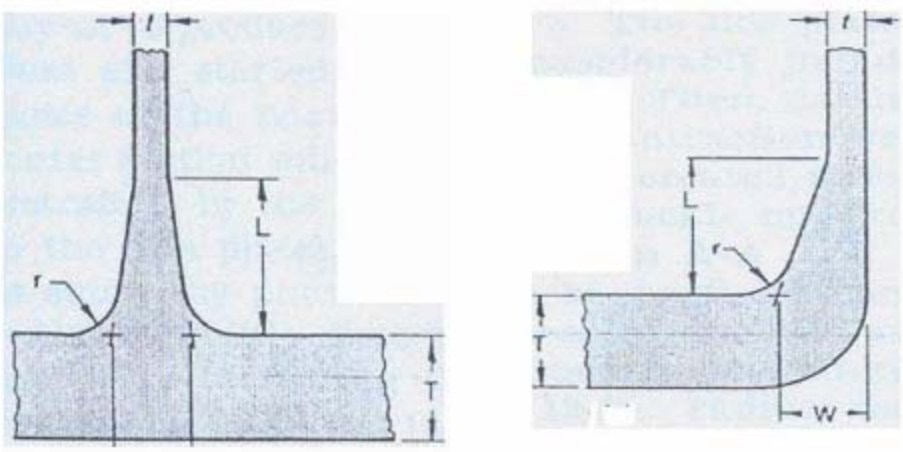

(a) Proper bending of T-junction (b) Proper bending of T-junction

corner.

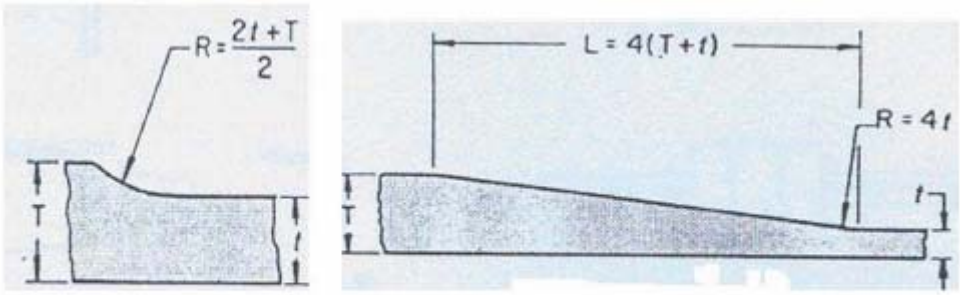

(c) Fillet if $\frac{T}{t} < 1.5$. (d) Blend if $\frac{T}{t} > 1.5$.

Figure 2.5: Unequal junctions (ASM, 1962)

Where T= thicker section, t=thinner section, L= length of taper

$$W = 0.75T \quad (2.1)$$

$$r = 0.50T \text{ (0.19 minimum)} \quad (2.2)$$

When $T/t > 4, L = 2T$ (2.3)

If $2 < T/t < 4, L = 1.5T$ (2.4)

Figures 2.5 (a) and (b) show recommended methods for blending abrupt changes in Thickness of a wall to minimize stress concentration. Figure 2.5 (c) shows a method Recommended where the thicker section is less than 50% larger than thin section. Figure 2.5 (d) shows a method recommended where thicker section is more than 50% larger than thin section. Casting is a complicated process, which involves considerable metallurgical and mechanical aspects. The rate of cooling governs the microstructure to a large extent,

which in turn controls the mechanical properties like strength, hardness and machinability.

The most probable location for shrinkage porosities inside a casting are Characterized by high temperature, coupled with low gradient and high cooling rate, so that to get temperature history it is important to understand solidification phenomenon.

2.2 Solidification Phenomenon

The solidification process involves the transformation of the hot liquid metal to solid and then subsequent cooling of the solid to the room temperature.

2.2.1 Assumptions

The following assumptions are made for the mathematical analysis of the solidification process (Venkatesen, et al., 2005; Huan, et al., 2004).

1. Contact resistance between the mould and cooling material is ignored.

2. In practice, the temperature difference between the mould surface and surrounding air is not high and radiation transfer can be ignored.

3. Mould cavity is instantaneously filled with molten metal.

4. Outer surface of the mould is initially assumed to be at ambient temperature.

5. The bottom surfaces of the casting are always in contact with the mold.

6. The vertical surfaces are in contact with the mould until air gap is formed.

2.2.2 Mathematical modeling

The field variables are the temperatures at all nodal points varying with the time (venkatesan, et al., 2005). Thermal properties like thermal conductivity, density, specific heat are also varying with temperature and hence the problem becomes non-linear transient in nature. As solidification progresses the metal shrinks causing an air gap formation between casting and mould. Heat transfer in the gap is due to convection only, and as the gap widens, the heat transfer coefficient is affected.

The governing equation of heat conduction in a moving fluid is given as (Sachdeva, 2000)

$$\rho c\left(\frac{\partial T}{\partial \tau}+u\frac{\partial T}{\partial x}+v\frac{\partial T}{\partial y}+w\frac{\partial T}{\partial z}\right)=\frac{\partial}{\partial x}\left(k_x\frac{\partial T}{\partial x}\right)+\frac{\partial}{\partial x}\left(k_y\frac{\partial T}{\partial x}\right)+\frac{\partial}{\partial x}\left(k_z\frac{\partial T}{\partial x}\right)+Q \quad (2.5)$$

In this expression Q represents the rate of heat generation. u, v, w are the velocities in the directions x, y, and z respectively. K, ρ, c are thermal conductivity, density and specific heat respectively.

Thus for stationary medium u = v = w = 0.

Now for unsteady state heat conduction, the equation reduces to,

$$\frac{\partial}{\partial x}\left(k_x \frac{\partial T}{\partial x}\right)+\frac{\partial}{\partial x}\left(k_y \frac{\partial T}{\partial x}\right)+\frac{\partial}{\partial x}\left(k_z \frac{\partial T}{\partial x}\right)+Q=\rho c\left(\frac{\partial T}{\partial \tau}\right) \quad (2.6)$$

The heat flow should also satisfy **boundary conditions**, which may be specified as Constant temperature at boundary or as known temperature gradient normal to the Boundary-specifying surface. In solidification of casting, Q is zero.

$T=T_0$ at S_1 surface. (2.7)

$$\frac{\partial T}{\partial n}=f(T) \text{ at } S_2 \text{ surface} \quad (2.8)$$

$$\text{or, } k\frac{\partial T}{\partial n}+\alpha T+q=0 \quad (2.9)$$

Where, s1 and s2 represents the portions of boundary on which these two boundary Conditions are specified. T and q are temperature and heat flux

Initial condition: It gives information of temperature at starting time. In this case

$$T=T_{01} \text{ at } \tau=0 \quad (2.10)$$

Boundary condition in different regions of casting and mold are given below (Ravi, 2005).

Solid-liquid interface: Rate of heat removed from the solid is equal to sum of rate of heat supplied to the interface by liquid and rate of heat supplied by liquid due to solidification.

$$-k_{sc}\frac{\partial T_{sc}}{\partial n}=-k_{lc}\frac{\partial T_{sc}}{\partial n}+\rho_{sc}L\frac{\partial S(\tau)}{\partial \tau} \quad (2.11)$$

.

Where, k_{lc} and k_{lsare} thermal conductivity for metal in liquid phase and in solid phase. L denotes latent heat, n denotes normal to the surface and S denotes the fraction solidified (that releases latent heat.)

Casting-mold interface: When there is no air gap, heat is transferred by conduction. Tc and Tm are temperature of mould and casting so that

$$\text{Heat flux} = k_c \frac{\partial T_c}{\partial n} = k_m \frac{\partial T_m}{\partial n} \qquad (2.12)$$

When air gap is formed the heat is transferred by convection and radiation. Heat flux is given by equation:

$$\text{Heat flux} = \sigma \varepsilon F\{(T_c + 273)^4 - (T_m + 273)^4\} + \alpha_g * \Delta T = -k\left(\frac{\partial T}{\partial n}\right) \qquad (2.13)$$

Where σ is Boltzmann's constant. ε is emissivity and F is form factor.

Outer surface of mold: Heat transfer by convection. Here Tmo is the temperature of outer surface of mould and Ta is ambient temperature.

$$\text{Heat flux} = -k_m \frac{\partial T_{mo}}{\partial n} = \alpha(T_{mo} - T_a) \qquad (2.14)$$

2.3 Physics Based Solidification Analysis

The major approaches used to solve solidification problems are finite element, finite Difference. The methods are briefly described below:

2.3.1 Finite difference method

It is assumed that material property does not vary with temperature and then heat transfer equation becomes:

$$K\left[\frac{\partial^2 T}{\partial x^2} + \frac{\partial^2 T}{\partial y^2} + \frac{\partial^2 T}{\partial z^2}\right] = \rho c \frac{\partial T}{\partial \tau} \qquad (2.15)$$

This equation can be solved by explicit finite difference method. In this method the casting and mold regions are subdivided into small intervals of constant space and time.

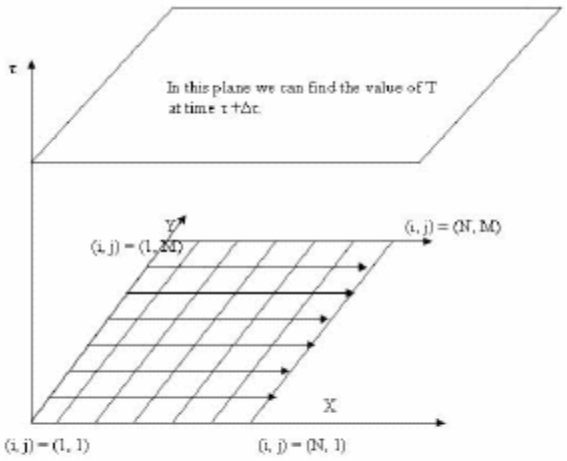

Figure 2.6: Space and time discretization in 2D

Solution of equation (2.15) by FDM:

$$\frac{T_{i,j,k}^{\tau+\Delta\tau}-T_{i,j,k}^{\tau}}{\Delta\tau}=\frac{k}{\rho c}\left(\frac{T_{i+1,j,k}^{\tau}-2T_{i,j,k}^{\tau}+T_{i-1,j,k}^{\tau}}{(\Delta x)^2}+\frac{T_{i,j+1,k}^{\tau}-2T_{i,j,k}^{\tau}+T_{i,j-1,k}^{\tau}}{(\Delta y)^2}+\frac{T_{i,j,k+1}^{\tau}-2T_{i,j,k}^{\tau}+T_{i,j,k-1}^{\tau}}{(\Delta z)^2}\right)+o(\Delta x_n)^2$$

Second term of right hand side is the truncation error. Equation 2.16 gives the solution of equation 2.15 in terms of temperature distribution with respect to space coordinates in casting and mold region, at desired time. The appropriate time step is determined by stability criterion which is given by,

$$\frac{k\Delta\tau}{\rho}\left(\frac{1}{(\Delta x)^2}+\frac{1}{(\Delta y)^2}+\frac{1}{(\Delta z)^2}\right)\leq\frac{1}{2} \qquad (2.17)$$

2.3.2 Finite element method

Heat transfer by conduction, convection and radiation plays vital role in many engineering applications (Gupta, 2000). The traditional approach to solve these problems relies heavily on providing the solution for highly simplified model, leaving the user to interpret an application to a realistic complex situation from the results. Often this approach does not work and prediction is far away from reality. The FEM takes care of these situations. There are two methods to solve the problem of heat flow:

1. Variational approach method

2. Weighted residue method.

In Variational approach method a function is always needed. Minimization of this

Function is equivalent to solving the governing equation of the problem. Euler- Lagrange equations form the basis of such formulation. It is not easy to find such a function.

In Weighted residue method the metal is assumed to be in complete contact with the mold surface (no air gap is formed) and it is also assumed that metal property does not vary in a particular element because it is very small. In this case, the transient heat conduction equation becomes,

$$K\left[\frac{\partial^2 T}{\partial x^2}+\frac{\partial^2 T}{\partial y^2}+\frac{\partial^2 T}{\partial z^2}\right]=\rho c\frac{\partial T}{\partial \tau} \qquad (2.18)$$

Boundary conditions

$T=T_0$ at s_1 for $\tau>0$.

$k\frac{\partial T}{\partial n}+\alpha T+q=0$ at s_2 for $\tau>0$.

By weighted residue method

$$\int_0^{\Delta\tau}\iiint_V\left[K\left(\frac{\partial^2 T}{\partial x^2}+\frac{\partial^2 T}{\partial y^2}+\frac{\partial^2 T}{\partial z^2}\right)-\rho c\frac{\partial T}{\partial \tau}\right]W_1 dv d\tau+\int_0^{\Delta\tau}\iint_S\left[K\frac{\partial T}{\partial n}+\alpha T+q\right]W_2 ds d\tau=0 \qquad (2.19)$$

T_1^1, T_2^1, T_3^1 etc are known temperature of nodes 1, 2, 3 at time $\tau=0$ and T_1^2, T_2^2, T_3^2 etc are unknown temperature at time τ_2.

$$T_1=N_1^1T_1^1+N_2^1T_1^2 \text{ and } T_2=N_1^1T_2^1+N_2^1T_2^2 \qquad (2.20)$$

Where N_1^1 and N_2^1 are shape function in time domain. Weighting function is a product of shape functions in space and time. We want to know temperature at τ_2 so that

$W_1=N_2^1N_i=-W_2$

$$\int_0^{\tau}\left[\int_V\left\{K\left(\frac{\partial^2 T}{\partial x^2}+\frac{\partial^2 T}{\partial y^2}+\frac{\partial^2 T}{\partial z^2}\right)-\rho c\frac{\partial T}{\partial \tau}\right\}N_i dv+\int_s\left(K\frac{\partial T}{\partial n}+\alpha T+q\right)N_i ds\right]N_2^1 d\tau=0 \qquad (2.21)$$

Considering 8-node brick element, the temperature within the element can be Expressed in terms of nodal temperature

$$T = \sum_{i=1}^{8} N_i T_i = [N][T^e] \tag{2.22}$$

$$\left[\int_V \left\{K\left(\frac{\partial^2 T}{\partial x^2}+\frac{\partial^2 T}{\partial y^2}+\frac{\partial^2 T}{\partial z^2}\right)-\rho c\frac{\partial T}{\partial \tau}\right\}N_i dv+\int_S\left(K\frac{\partial T}{\partial n}+\alpha T+q\right)N_i ds\right]=[H]\{T\}+[C]\frac{\partial\{T\}}{\partial \tau}+\{F\}$$

Where [H] and [C] are conductivity matrix and capacitance matrix, and {F } *F* is load vector. So the equation reduces to

$$\int_0^{\Delta\tau} N_2^1\left[[H]\{T\}+[C]\frac{\partial\{T\}}{\partial \tau}+\{F\}\right]d\tau = 0 \tag{2.24}$$

If τ1=0 and τ2=Δ τ then after integration,

$$\{T^2\} = -\left[\frac{2}{3}[H]+\frac{1}{\Delta\tau}[C]\right]^{-1}\left\{\left[\frac{1}{3}[H]-\frac{1}{\Delta\tau}[C]\right]\{T^1\}+\{F\}\right\} \tag{2.25}$$

Coincident node technique: It is known that air gap is formed between casting and Mould. For solving this type of problem coincident node technique (Robinson, et al., 2001) is used. In this technique, the interfacial heat transfer coefficient (IHTC) is used to account for the heat transfer from casting to mold. This depends on the air gap between casting and mould. For an element having convective heat transfer across its face, the conductivity matrix acquires an additional term. This additional term gives the conductivity matrix for the virtual gap element. Hence, along with the casting elements and mold elements, a third type of element group, namely, gap elements are used in the FE modeling of metal solidification process (Samonds, et al., 1985).

The rate of heat transfer is given by

$$q = A\int_A \alpha_g (T_c - T_m)dA \tag{2.26}$$

Where,

Tc and Tm are the temperatures on the casting side and mould side. α*g* is Interfacial heat transfer coefficient, accounts for heat flux from casting to mould by

Convection, conduction and radiation. In figure 2.7, node c1 and m1, c2 and m2, c3 and m3, c4 and m4 are the coincident nodes on the interface.

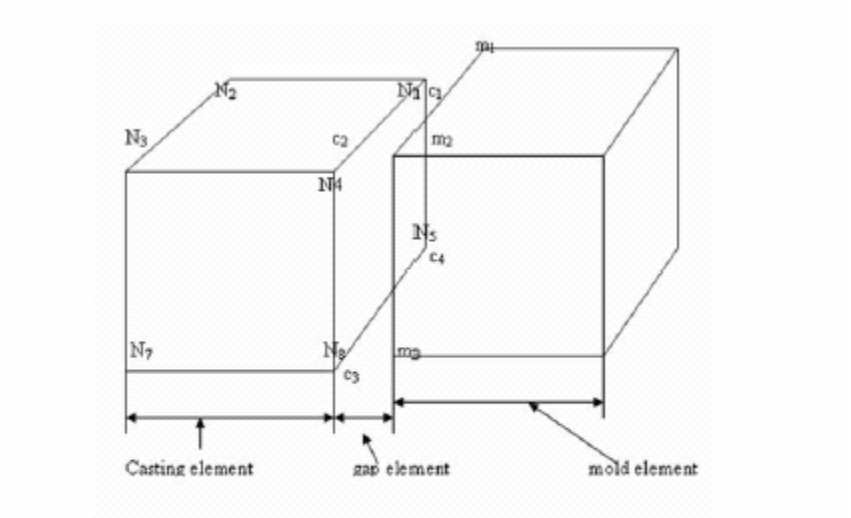

Figure 2.7: The gap element arrangement

For an element lying on the casting side with one face exposed to gap, the weighted residue equation can be written as:

$$\int_V \begin{Bmatrix} \frac{\partial T}{\partial x} \\ \frac{\partial T}{\partial z} \\ \frac{\partial T}{\partial z} \end{Bmatrix} \begin{bmatrix} k & 0 & 0 \\ 0 & k & 0 \\ 0 & 0 & k \end{bmatrix} \begin{Bmatrix} \frac{\partial w}{\partial x} \\ \frac{\partial w}{\partial y} \\ \frac{\partial w}{\partial z} \end{Bmatrix} dV + \int_V \rho c \frac{\partial T}{\partial \tau} w dV + \int_A \alpha (T_c - T_m) w dA = 0 \qquad (2.27)$$

Where, $T_c = \sum_{i=1}^{n} N_i(+1, s, t) T_i^c$, and $T_m = \sum_{i=1}^{n} N_i(-1, s, t) T_i^m$

The shape functions in the form local co-ordinate system (ξ, η, ζ) are as follows (Venkatesan, et al., 2005):

$$\begin{aligned} N_1 &= (1+\xi)(1+\eta)(1-\varsigma)/8 \\ N_2 &= (1-\xi)(1+\eta)(1-\varsigma)/8 \\ N_3 &= (1-\xi)(1-\eta)(1-\varsigma)/8 \\ N_4 &= (1+\xi)(1-\eta)(1-\varsigma)/8 \\ N_5 &= (1+\xi)(1+\eta)(1+\varsigma)/8 \\ N_6 &= (1-\xi)(1+\eta)(1+\varsigma)/8 \\ N_7 &= (1-\xi)(1-\eta)(1+\varsigma)/8 \\ N_8 &= (1+\xi)(1-\eta)(1+\varsigma)/8 \end{aligned} \qquad (2.28)$$

Now Ni can be denoted in the form of r, s, t. the gap element does not posses

capacitance matrix and the load vector. While calculating the shape function, r= +1 is taken for casting and r= -1 is taken for mold.

2.4 Geometry Based Modeling

The other approach of analyzing solidification is based on the geometry of part. This includes inscribed circle, modulus, and vector element method, which are described below:

2.4.1 Circle method

Inscribed circle is used to compare different section of casting. The ratio of the area of the inscribed circles is indication of relative freezing times. The large sections finish freezing proportionately later than the small section.

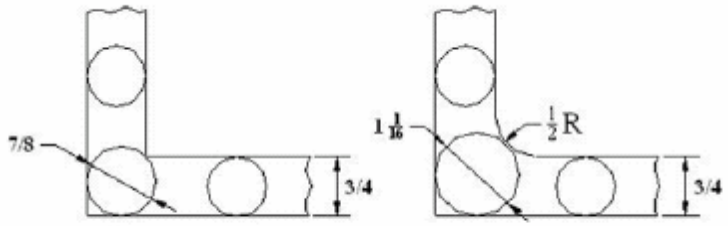

Figure 2.8: Inscribed circles facilitate comparison of metal mass in casting junction

By figure 2.8, it can be seen that result of fillet is increase in mass. The ability of
The sand or ceramic mold to absorb heat must be considered when junctions are being Designed. In general, heat from molten metal is transferred into the mold in the direction perpendicular to the interface or in radial direction if the interface is curved. In a junction, at outer surface large amount of mould material is available compared to inner surface. So that outer corner will cool faster compare to inner corner. If there is no other feeding arrangement then shrinkage defect will result. When fillet is provided at the corner the shrinkage cavity will reduce. If fillet radius is equal to the wall thickness of the junction members of the casting, shrinkage voids are usually eliminated.

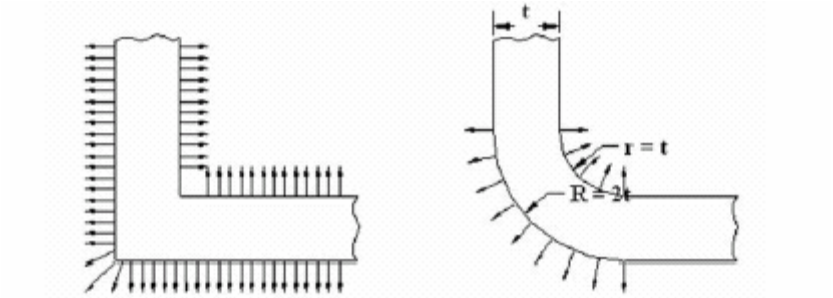

Figure 2.9: Direction of heat transfer from solidifying metal to mold

2.4.2 Modulus method

The following assumptions are made for deriving an equation for solidification time of a simple shaped casting:

1. Flow of heat is unidirectional, and the mold is semi-infinite (that is, neglect the effect of finite thickness of mold).

2. The properties of the metal and mold material are uniform (throughout the bulk) and remain constant over the range of temperature considered.

3. The metal is in complete contact with the mold surface (no air gap is formed).

4. The metal-mold interface temperature remains constant from the start to end of the solidification.

The solidification time τs can be determined by equating the heat given up by the casting Qcast to the heat transferred through the mold Q mold.

$$Q_{cast} = \rho_{cast} V[L + C_{cast}(T_{pour} - T_{sol})] \quad (2.29)$$

$$Q_{mold} = 1.128\sqrt{(K_{mold}\rho_{mold}C_{mold})}(T_{int} - T_{amb})A\sqrt{\tau_s} \quad (2.30)$$

Equating both equations, we obtain Chvorinov's equation (Ravi, 2005)

$$\sqrt{\tau_s} = (\rho_{cast}(L + C_{cast}(T_{pour} - T_{sol})))/(1.128\sqrt{(K_{mold}\rho_{mold}C_{mold})}(T_{int} - T_{amb}))(V/A))$$

$$\tau_s = \mathrm{K}\,(\mathrm{V/A})^2 \quad (2.32)$$

Where V is the casting volume (representing the heat content) and A is the cooling surface area (through which heat is extracted). The ratio V/A is referred to as the casting modulus.Let two different shapes have same volume (say, a cube and plate). The one with the larger cooling surface area (plate) will solidify first. This method can be used to determine the order of solidification of different regions of casting, by dividing it into simple shapes and determining the volume and cooling surface area of each region. The region with the

highest modulus is considered to solidify last and identified as a hot spot. Feeders are designed so that their modulus is more than the modulus of hot spot region. Due to this feeder remains liquid and compensate the volumetric shrinkage.

2.4.3 Vector element method

This method is used to determine feed path and hot spot inside the casting. The feed path is assumed to lie along the maximum thermal gradient. By Fourier's law, (Ravi, 2005)

$$Q=-kA\,(\Delta T/\Delta s) \qquad (2.33)$$

$$G=(-1/k)\,q \qquad (2.34)$$

Where, $G = (\Delta T/\Delta s)$ is thermal gradient and $q = Q/A$ is the heat flux at any given point inside the casting, in any given direction. Gradient is zero in tangential direction to isotherm and maximum perpendicular to isotherm at any point inside the casting. The magnitude and direction of the maximum thermal gradient at any point inside the casting is proportional to the vector result of thermal flux vectors in all directions originating from that point.

$$q_r=\sum q_i \qquad (2.35)$$

The casting volume is divided into a number of pyramidal sectors originating from the given point, each with small solid angle. A step is taken along resultant flux vector, reaching a new location and repeating the computation, until the resultant heat flux is zero. The final location is the hot spot. The locus of points along which iterations are carried out is the feed path.

2.5 Summary

• Junctions are intersection of two or more casting sections. There are five types of junctions: L, T, V, X, Y. Main parameters of casting design are thickness, angle and fillet radius.

• Tapered fillets are required in an area where the junctions can serve as flow and feed path for molten metal.

• Junction design guidelines are based upon equal section and unequal section. Size of defects can be eliminated or decreased by proper selection of fillet radius and coring a hole in case of equal sections. In case of unequal section, by gradual increase of thickness of thin section gives equal section at juncture. It also helps to solve the problem of stress concentration.

• The solidification process involves the transformation of the hot liquid metal to solid and then subsequent cooling of the solid to the room temperature.

• Material properties like density, thermal conductivity and specific heat vary with temperature which varies with time. So problem is non-linear transient in nature.

• There are two types of solving techniques one is based on physics and other is based on geometry alone.

• Physics based methods include FDM, and FEM. Both methods give nodal temperature where the casting and mold region is divided into intervals of time and space. FDM and FEM discretize the volume into number of elements.

• Geometry based methods are circle method, modulus method and VEM. These methods are very simple and give approximate result. In circle method, the diameter of circle indicates relative solidification time. Modulus method is a practical approach based on several assumptions. VEM gives full information of feed path and finally leads to hot spot, the region of shrinkage defect.

• 2D Solidification analysis of junctions gives the temperature at each and every node, which is used to calculate thermal gradient and solidification rate which finally helps to predict size and shape of shrinkage cavity.

Chapter 3

Problem Definition

A main problem of a junction is metal shrinkage. Thin sections will freeze before heavy section and can freeze first and shut off the source of feed metal for heavy section. Hence there will be no source of feed metal to replace the volume lost because of metal shrinkage; such a heavy section will be porous. The most probable locations for shrinkage porosity inside a casting are characterized by high temperature, coupled with low gradient and high cooling rate.

• High temperature signifies fewer directions from where liquid metal can flow in to compensate for solidification shrinkage.

• Low gradient implies that even if liquid metal is available at a neighboring region, there is insufficient thermal pressure for the flow to actually take place.

• High cooling rate implies that even if liquid metal and sufficient gradients are available, the time available is too short and the liquid metal freezes before reaching the hot spot.

3.1 Objectives

The goal of this project was to build a simple mathematical model for prediction of Shrinkage porosity in casting junctions as a function of junction design parameter based on a study of experimental work and casting solidification simulation. The detailed objectives are as follows:

1. Collect and collate existing literature (mainly design guidelines based on experimental analysis) related to junctions.

2. Identify the junction design parameters.

3. Create 2D models of typical junctions and carry out solidification analysis using both geometry and physics based methods.

4. Identify good and bad designs of junctions (considering solidification shrinkage) based upon above studies.

5. Build a set of design guidelines and empirical equations for quick prediction of shrinkage problem in quick junctions.

3.2 Approach

This approach involved analysis of the junction and identification of the junction design parameters. Analysis has done for 2D models with varying junction design parameters like thickness, angle and fillet radius. Solidification analysis was carried out with the help of physics and geometry based methods. This will lead to identification of good and bad design. Good design contained small area of shrinkage defect and bad design contained large area of defect. These defects helped in generation of empirical equation.

Chapter 4

Prediction of Shrinkage Cavity

4.1 Introduction

There is an increasing demand in the metal casting industry for a reliable and easy method of shrinkage prediction as one of the means of competing with other branches of manufacturing. Great savings of materials, energy and time will be achieved, if casting design can be corrected prior to moulding on the basis of shrinkage prediction. Such predication is particularly desirable for large steel castings, which are normally produced in a small number and hence, the failure of first trial means a relatively large loss when compared to castings that are mass produced.

The solidification process involves the transformation of the hot liquid metal into solid and then subsequent cooling of the solid up to room temperature. Solidification analysis of junctions helps in prediction of shrinkage area. Shrinkage porosity formation is a complex phenomenon involving at least heat flow and liquid metal flow as governing factors. There are three methods to predict shrinkage porosity.

On the basis of solid fraction ratio: It is formed due to interdendritic molten metal flow. The microscopic fluidity of molten metal exists in the region where the solid fraction ratio is less than the critical solid fraction ratio fcr=0.67. Shrinkage cavity is always generated within the fcr loop. fcr loop shrinks in the solidification process. At ultimate moment when fcr loop disappears, it coincides with final generation portion of the shrinkage cavity (Imafuku, et al, 1983).

On the basis of thermal gradient: This is pure heat flow analysis, but it gives information more directly related to metal flow. Mapping of the calculated temperature gradient at the time of solidification is found to be a powerful tool for predicting shrinkage porosities in actual casting. Shrinkage porosities in actual castings are found in those areas where the temperature gradient at the time of solidification is calculated to be below 200 degree per meter (Niyama, et. al., 1981).

On the basis of thermal gradient and rate of solidification: Shrinkage porosities in actual castings are found in those areas where ratio of thermal gradient (G) in Kelvin/sec and square root of solidification rate (R) in mm/s is less than 1 (Chen, et al., 1990).

$$\frac{G}{\sqrt{R}} < 1 \qquad (4.1)$$

4.2

4.2Critical Solid Fraction Ratio

Solid liquid region is first divided into two sub regions p and q, as shown in figure 4.1. In the p region, the fluidity of the molten metal within the dendrite structure does not exist, however, the molten metal in q region can move downwards by the force of gravity. Then the solid fraction ratio at boundary of p and q sub-regions is termed as the critical solid fraction ratio, fcr.

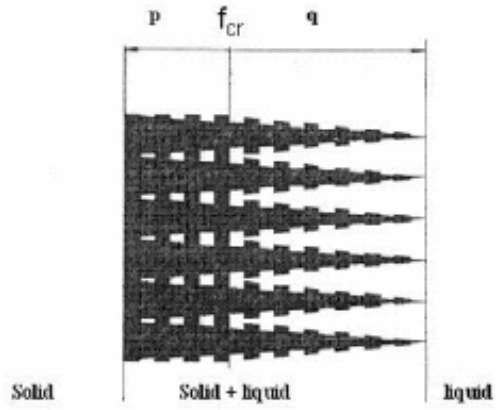

Figure 4.1: Dendrite structure (Imafuku, et al., 1983)

4.3 Formulation of Solid Fraction Ratio

This section proposes a formulation which enables quantitative evaluation of solid fraction ratio as a function of temperature. Since the prediction method of shrinkage cavity is based upon solid fraction ratio, the accuracy of method depends on that calculated solid fraction ratio. The solid fraction ratio fs is formulated as a function of temperature by utilizing the Fe-C diagram. The mixture of solid and liquid region is approximated by straight lines. The modified Fe-C diagram is shown in figure 4.2, where

m1, m2, k1, and k2 are constants and are used to represent straight lines as shown in

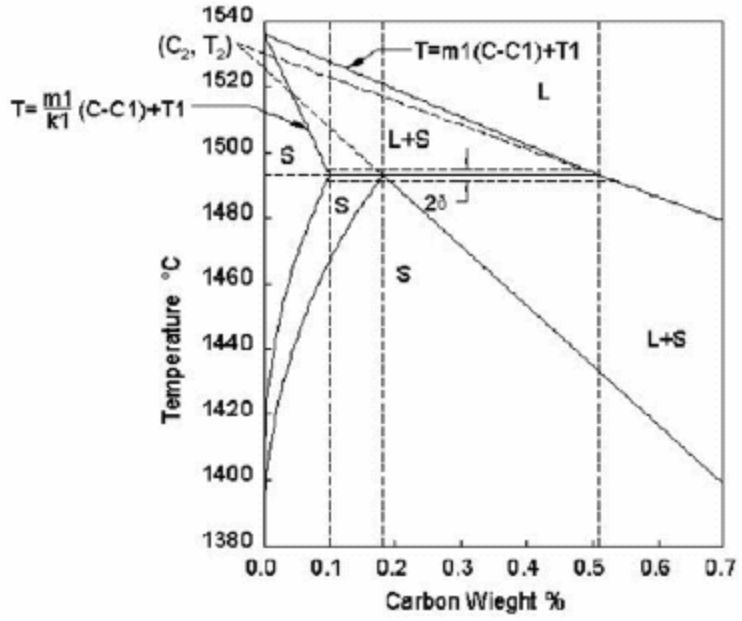

Figure 4.2: Approximated Fe-C Equilibrium diagram

figure 4.2.

Equilibrium diagram is composed of four regions, as follows:

1) $0.00 \leq C \leq 0.10$ (wt %)

2) $0.10 \leq C \leq 0.18$ (wt %)

3) $0.18 \leq C \leq 0.51$ (wt %)

4) $0.51 \leq C$ (wt %)

It is assumed that solid fraction ratio fs linearly vary with temperature. The solidus and liquidus lines can be represented as Line1 and Line2 as shown in figure 4.3. Let P(C2,T2) and Q(C3,T3) points lie on Line1 and Line2 respectively where T represents the temperature and C represents the carbon %. The line PQ is called tie-line.

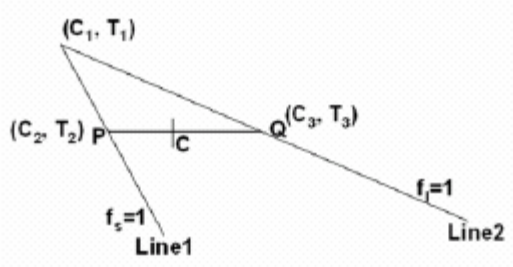

Figure 4.3: Fe-C equilibrium diagram above eutectic temperature

For Line1:

$$T = m_1(C - C_1) + T_1 \tag{4.2}$$

$$T_2 = m_1(C_2 - C_1) + T_1$$

$$C_2 = \frac{(T_2 - T_1)}{m_1} + C_1 \tag{4.3}$$

For Line2:

$$T = \frac{m_1}{k_1}(C - C_1) + T_1 \tag{4.4}$$

$$T_3 = \frac{m_1}{k_1}(C_3 - C_1) + T_1$$

$$C_3 = \frac{(T_3 - T_1)k_1}{m_1} + C_1 \tag{4.5}$$

By lever's law solid fraction ratio at the tie line PQ can be found as

$$f_s = \frac{(C - C_3)}{(C_2 - C_3)} \tag{4.6}$$

$$f_s = \left[1 - \frac{(C - C_1)m_1}{(T - T_1)}\right]\frac{1}{(1 - k_1)} \tag{4.7}$$

Eutectic region exists within the range of $0.10 \leq C \leq 0.51$, which is shown in figure 4.4. Present study assumes that fs varies linearly within a small temperature range of 2δ with the centre defined as Tp. M and N are two points lie in Eutectic region as shown in figure 4.4.

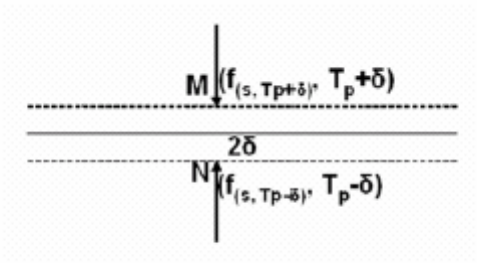

Figure 4.4: Fe-C equilibrium diagram at eutectic temperature

Equation of line MN is

$$f_s = \frac{1}{2\delta}\left[f_{(s,T_p-\delta)}\{(T_p+\delta)-T\} - f_{(s,T_p+\delta)}\{(T_p-\delta)-T\}\right] \quad (4.8)$$

$$f_{(s,T_p-\delta)} = 1$$

$$f_{(s,T_p+\delta)} = \left[1-\frac{(C-C_1)m_1}{(T_p+\delta-T_1)}\right]\frac{1}{(1-k_1)} \quad (4.9)$$

$$f_s = \frac{1}{2\delta}\left[f_{(s,T_p-\delta)}\{(T_p+\delta)-T\} - \frac{1}{1-k_1}\left\{1-\frac{m_1(C-C_1)}{T_p+\delta-T_1}\right\}\{(T_p-\delta)-T\}\right] \quad (4.10)$$

For 0-0.18 % of carbon fs can be calculated using of equation 4.7. As eutectic region exists between 0.1 to 0.18 % of carbon, the formulation is divided into two parts, as follows:

• (Tp+δ)< T≤ Tl : In this region, fs is calculated by 4.7.

• (Tp-δ)≤ T≤ (Tp+δ): In this region, fs is calculated by 4.10.

There are 3 parts for 0.18 to 0.51 % of carbon, as follows:

• (Tp+δ)< T≤ Tl: In this region, fs is calculated by 4.7.

• (Tp-δ)≤ T≤ (Tp+δ): In this region, fs is calculated by formula 4.11.

$$f_s = \frac{1}{2\delta}\left[\frac{1}{(1-k_2)}\left\{1-\frac{m_2(C-C_2)}{(T_p-\delta)-T_2}\right\}\{(T_p+\delta)-T\} - \frac{1}{1-k_1}\left\{1-\frac{m_1(C-C_1)}{T_p+\delta-T_1}\right\}\{(T_p-\delta)-T\}\right] \quad (4.11)$$

• (Tp+δ) ≤ T≤ Ts: In this region, fs is calculated by formula 4.12.

$$f_s = \left[1-\frac{(C-C_2)m_2}{(T-T_2)}\right]\frac{1}{(1-k_2)} \quad (4.12)$$

fs for more than 0.51 % of carbon are calculated by equation 4.12. Next section

explains the analysis carried out with material composition as shown below in table 4.1. Figure 4.5 Represents Line1 and Line2 with co-ordinates

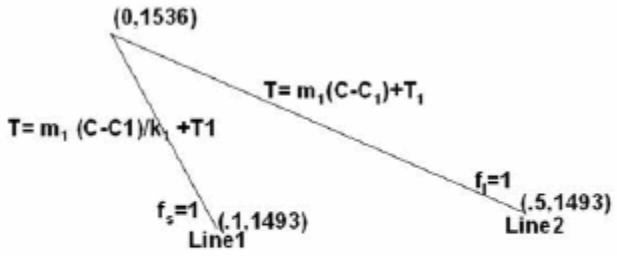

Figure 4.5: Fe-C equilibrium diagram above eutectic temperature with co-ordinates.

Table 4.1: Material compositions (Imafuku, et al., 1983)

Element	C	Si	Mn	P	S
Wt%	0.098	0.43	0.78	0.012	0.010

m1 = -86 and k1=0.2 is produced by comparing equation of Line 1 and 2 with actual equations. So that

$$f_s = \left[1 + \frac{86C}{(T-1536)}\right] * \frac{1}{0.8} \qquad (4.13)$$

For C= 0.098% (wt)

$$f_s = \left[1.25 + \frac{10.5}{(T-1536)}\right] \qquad (4.14)$$

Transient heat transfer analysis during solidification is carried out by finite element method (FEM) technique. Commercial software ANSYS is used, which gives nodal temperature. These temperatures will be used to find critical solid fraction ratio (fcr).

4.4 Analysis of Junctions using ANSYS

Two-dimensional geometry of typical junctions is analyzed using ANSYS 6.0. The analysis is carried out in three steps as below:

• ***Preprocessing:*** used to define geometry, material property, and element type for the

analysis.

• ***Solution*:** phase defines analysis type like transient or steady state, apply loads and solve the problem.

• ***Postprocessing*:** is to review the result in the form of graphs or tables. The general postprocessor is used to review results at one sub step (time step) over the entire model. The time-history postprocessor is used to review results at specific points in the model over all time steps.

The following assumptions are made for the analysis:

1. Contact resistance between the mold and cooling material is negligible.

2. In practice the temperature difference between the mould surface and surrounding air is not substantial hence radiation transfer can be ignored.

3. Mould cavity is instantaneously filled with molten metal.

4. Outer surface of the mould is initially assumed to be at ambient temperature.

5. The bottom surfaces of the casting are always in contact with the mould.

6. The vertical surfaces of casting are in contact with the mould i.e. no air gap in between.

4.4.1 Modeling of Junction

In ANSYS, model generation means generation of nodes that represent the spatial volume. Modeling consists of defining two parts one is sand mould and other is the castings with proportional dimensions. The minimum distance between the mould and casting must be sufficient to prevent damage to the mould during handling and casting. The minimum distance ranges from 25mm for small castings to 200mm or more for large casting. One such model is shown in figure 4.6.

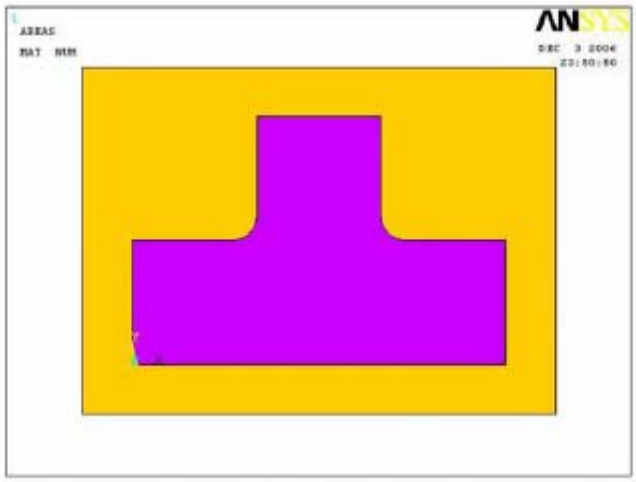

Figure 4.6: Model of T-section using ANSYS

4.4.2 Meshing

The main aim of the analysis is to get temperature distribution with respect to time. Element, PLANE 55 is chosen in ANSYS which has capability of transient heat transfer analysis. The element has four nodes with a single degree of freedom, temperature, at each node. PLANE 55 is a four node quadrilateral element with linear shape functions.Complete mesh model of T-section is shown in figure 4.8.

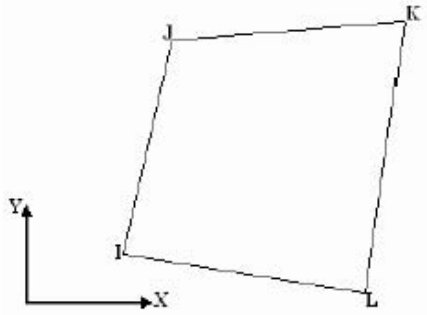

Figure 4.7: PLANE55 element

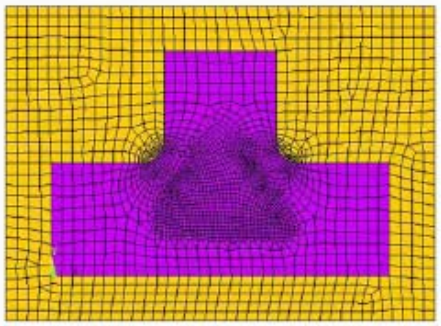

Figure 4.8: Mesh model of T-section

4.4.3 Input to ANSYS model

In present work, analysis is carried out for the time from pouring temperature to solidification temperature. Solidification time varies with respect to dimension. Input parameters provided for ANSYS model are as follows:

1. Initial boundary conditions:

• Sand mould is at room temperature 250 C.

• Casting is poured at 15800 C.

2. Thermal boundary condition are as follows (Venkatesan, et al.,2005):

• Convective heat transfer coefficient =12 W/m2-k.

• Bulk temperature of ambient air = 250 C.

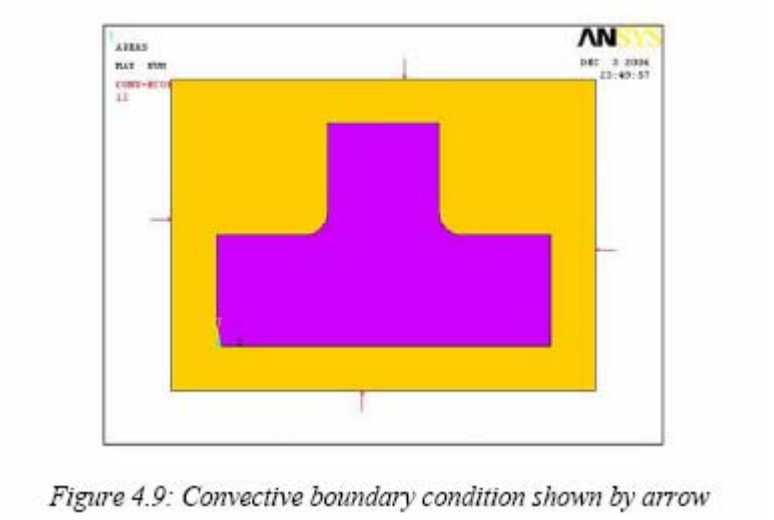

Figure 4.9: Convective boundary condition shown by arrow

3. Material specifications considered are as follows (Imafuku, et al., 1983):

• Chemical composition as shown in table 4.1.

• Density of steel in solid state = 7500 kg/m3.

• Density of steel in liquid state =7000 kg/ m3.

• Density of sand = 1520 kg/m3.

• Material properties like thermal conductivity, enthalpy, and specific heat vary with temperature. Figure 4.10 and 4.11 represent sand and steel properties.

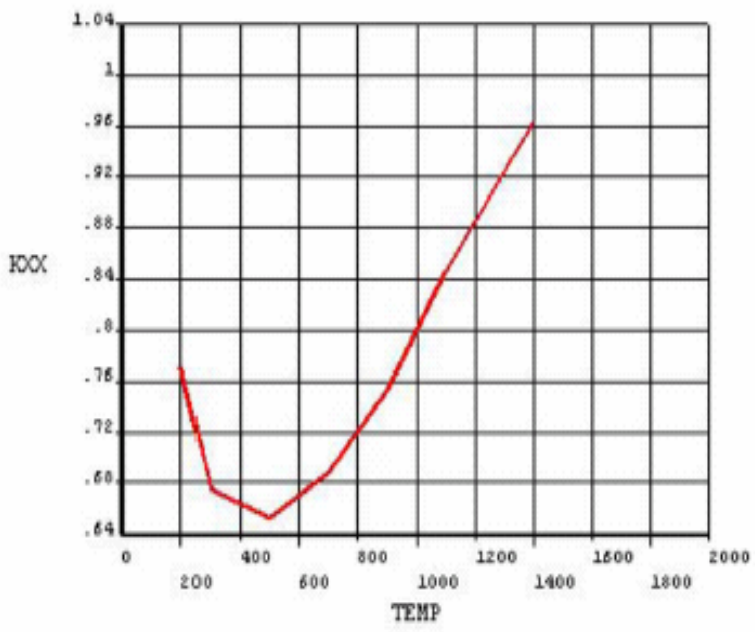

Figure 4.10a: Variation of thermal conductivity of sand with respect to temperature

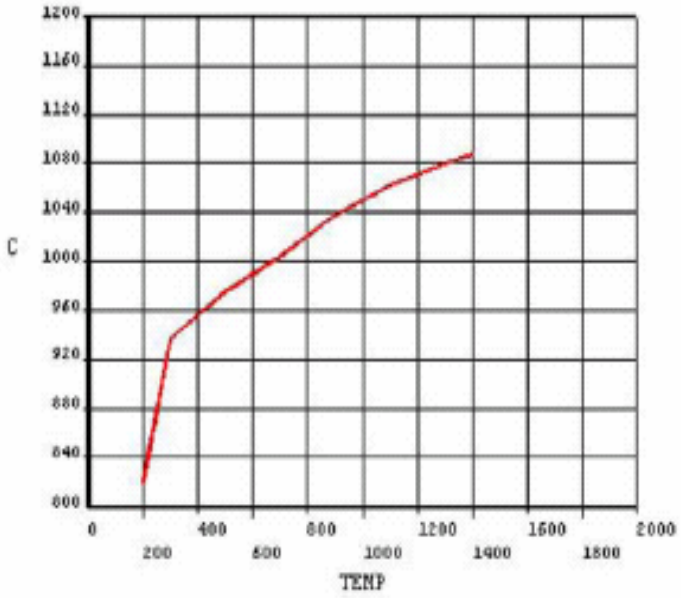

Figure 4.10b: Variation of specific heat of sand with respect to temperature

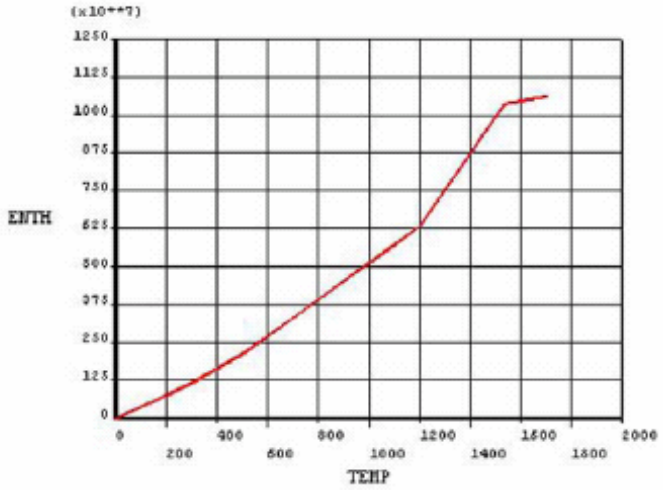

Figure 4.11a: Variation of specific enthalpy (J/m^3) of steel with respect to temperature

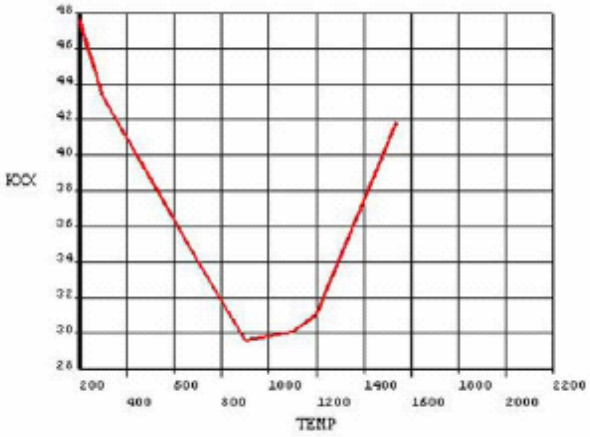

Figure 4.11b: Variation of thermal conductivity of steel with respect to temperature

4.4.4Locating Shrinkage Cavity by Solid Fraction Ratio

As the carbon is 0.098% (wt), the formula used for calculation of solid fraction ratio is equation 4.14. But fcr required for formulation of shrinkage cavity is 0.67. By equation 4.14,

$$f_s = \left[1.25 + \frac{10.5}{(T - 1536)}\right]$$

$$0.67 = \left[1.25 + \frac{10.5}{(T - 1536)}\right], \text{ So that, T=1517.89}^0 \text{ C}$$

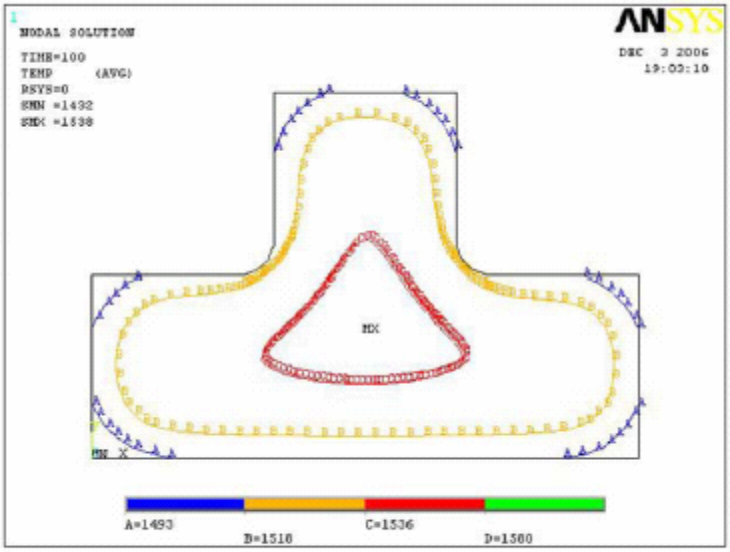

Figure 4.12a: Temperature distribution in T-junction after 100 sec.

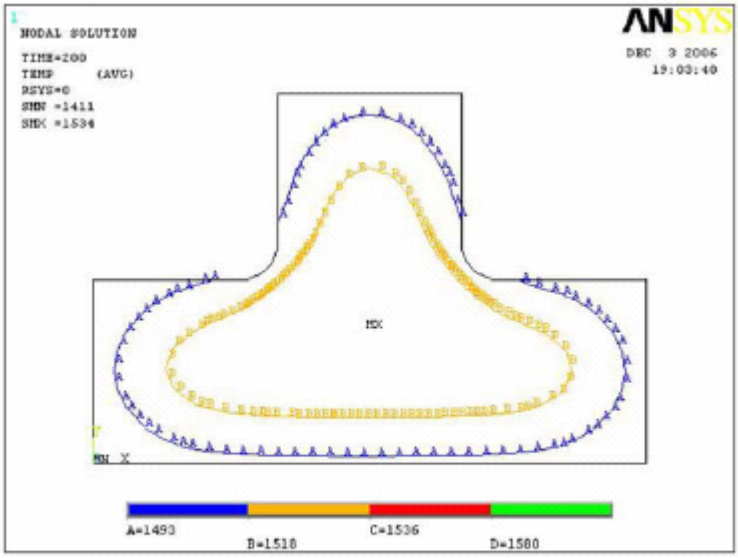

Figure 4.12b: Temperature distribution in T-junction after 200 sec.

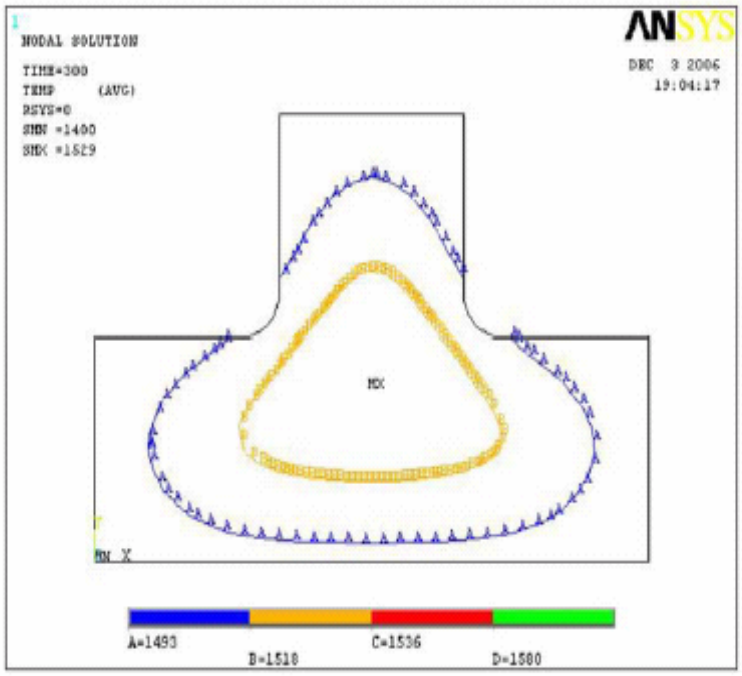

Figure 4.12c: Temperature distribution in T-junction after 300 sec.

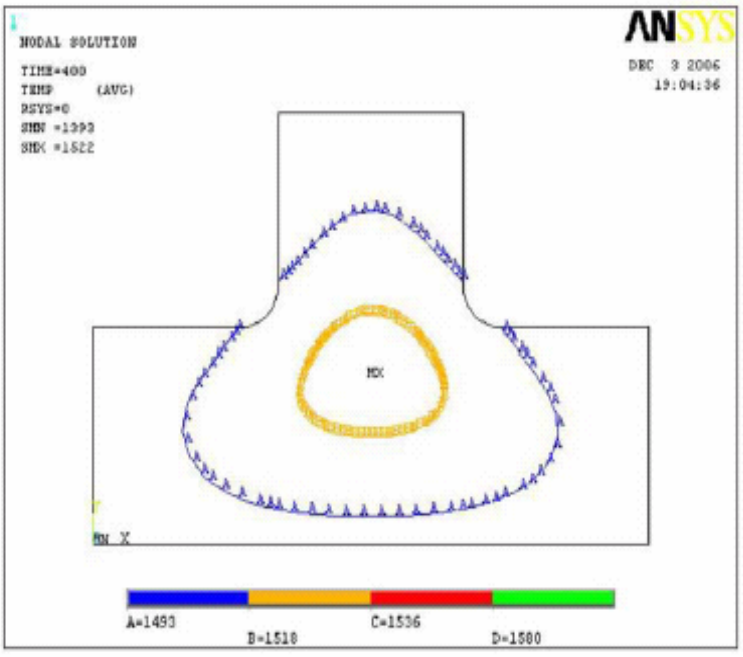

Figure 4.12d: Temperature distribution in T-junction after 400 sec.

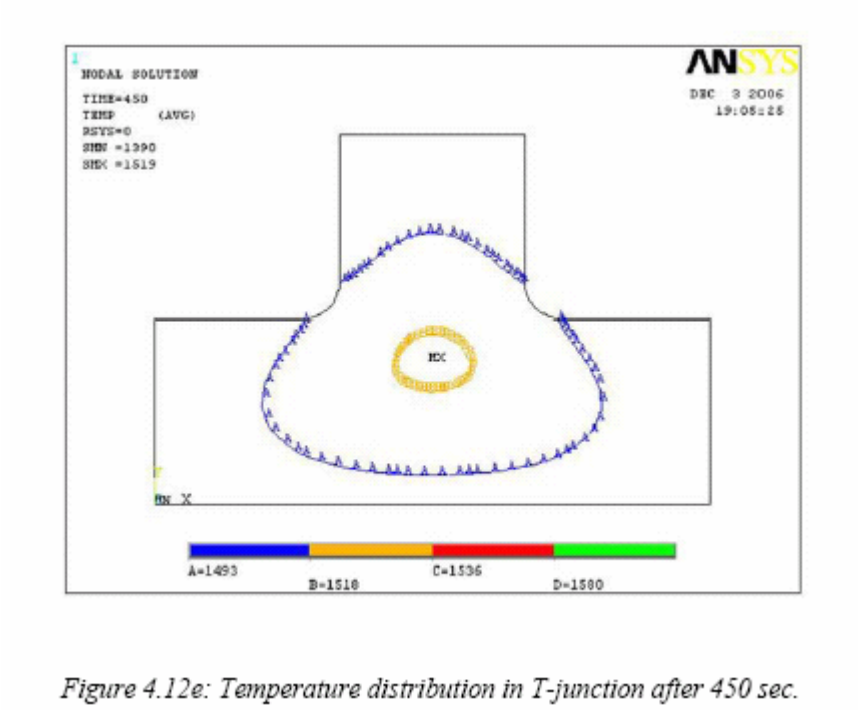

Figure 4.12e: Temperature distribution in T-junction after 450 sec.

Figures 4.12 (a, b, c, d, e) represent temperature distribution of T- junction with respect to time. In these figures temperature 1518° C is represented by B. As per expectation, it shrinks with respect to time and after 450 sec (approx.) it disappears. Node number and coordinate of those nodes which are passing through line B are found out and used for the calculation of shrinkage volume. The resultant shrinkage cavity formed is shown in figure 4.13.

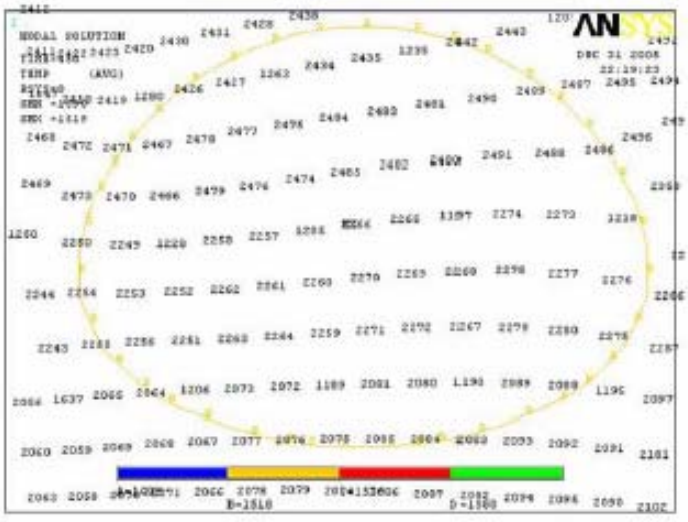

Figure 4.13: Shrinkage cavity by solid fraction ratio

4.4.5 Locating Shrinkage Cavity by Gradient Method

It has been experimentally established that shrinkage appears in a region where the temperature gradient is low at the time of solidification. In fact practically, all of the shrinkage is found within the region of calculated temperature gradient of 2000/m. therefore 2000/m is tentatively taken as the limit for shrinkage appearance.

The thermal gradient Gij between two points i and j inside the casting at given instant of time is given by

$$G_{ij} = \frac{(T_j - T_i)}{\Delta S} \qquad (3.15)$$

Where $T_i - T_j$ is the difference in temperature between the two points and $S\,\Delta$ is the distance between them. The gradients are greatly influenced by the casting geometry. In general, the gradients are highest in a direction normal to the solidification front, gradually decreases from mould to the casting centre.

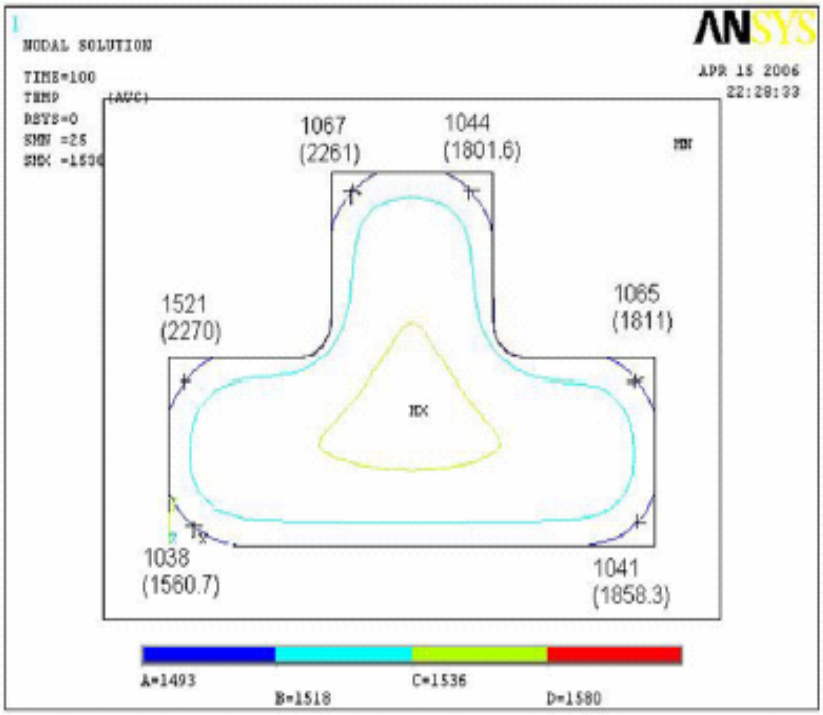

Figure 4.14a: Thermal gradients on the solidification contour after 100 sec.

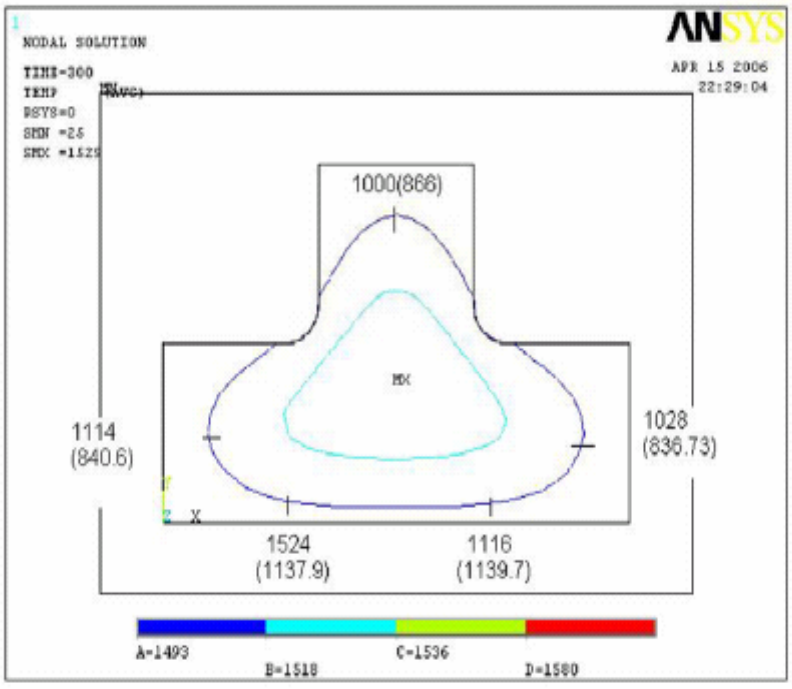

Figure 4.14b: Thermal gradients on the solidification contour at 300 sec.

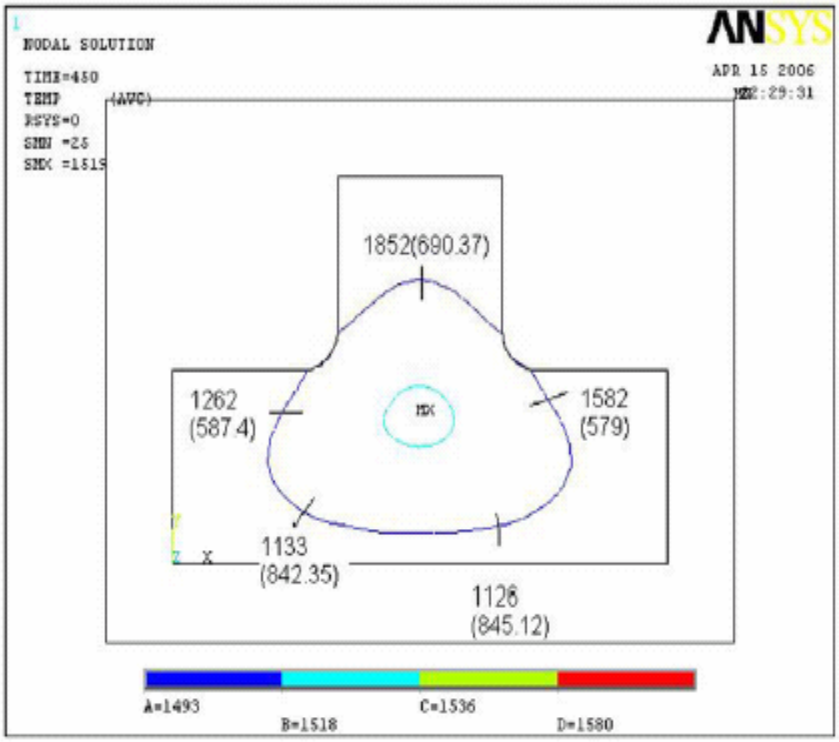

Figure 4.14c: Thermal gradients on the solidification contour at 450 sec.

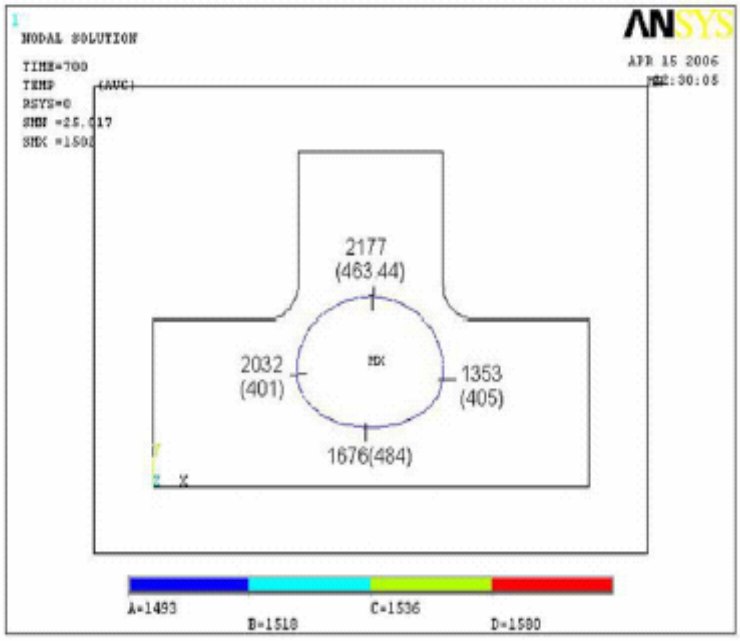

Figure 4.14d: Thermal gradients on the solidification contour at 700 sec.

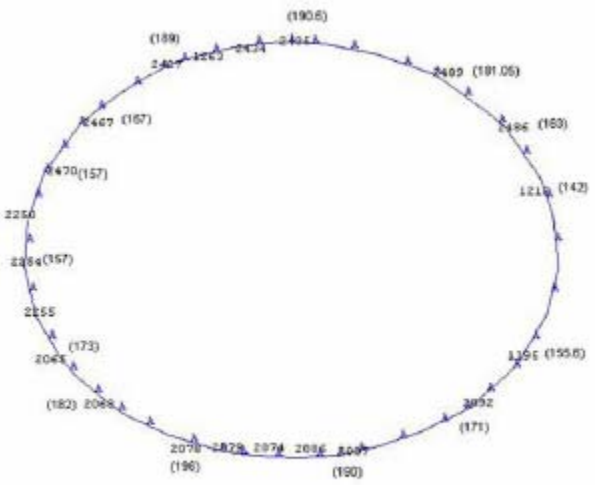

Figure 4.14e: Shrinkage cavity by thermal gradient

In figure 4.14a, line A (blue line) represents solidification contours, bracketed numbers (2261, 1801.6, 1811,1858.3,1560.7 and 2270) represent thermal gradient with respect to corresponding node numbers (1067, 1044, 1065, 1041, 1038 and 1521). As per expectation, thermal gradient at solidification contour decreases with respect of time, as shown in figure 4.14 (a, b, c and d). In figure 4.14e, thermal gradient at all nodes are below2000/m so it represents required shrinkage volume. By using co-ordinate of node, shrinkage volume can be calculated.

4.5 Summary

• There are mainly three methods for the prediction shrinkage cavity based upon solid fraction ratio, thermal gradient and solidification rate.

• Solid fraction method: At ultimate moment when critical solid fraction ratio (fcr=0.67) loop disappears, it coincides with final generation portion of the shrinkage cavity.

• Thermal gradient method: Shrinkage porosities in actual castings are found in those areas where the temperature gradient at the time of solidification is calculated to be below 200 degree per meter.

• Temperatures of each and every location are required for calculation of solid fraction ratio and thermal gradient, so that finite element method is used to solve the transient heat transfer problem.

Chapter 5

Results and Discussion

5.1 Introduction

Molten metal at the junctions does not possess sufficient surface area for the cooling purpose, and mould sand, a poor conductor of heat cannot conduct the heat away from the sand enclosed between the sections of casting as quickly as the heat is transferred from the molten metal into this mould section, so that shrinkage defect occurs inside the junction. In case of junction, hot spot is readily developed in the mould at junction. Main motto in junction design is more increase in surface area as compare to increase in volume, where numbers of sections meet each other.

5.2 L-Junction

Shrinkage cavity for L-junction are shown in figure 5.1, they belong to serial number 14, 15 and 16 in table 5.3 with their dimensions are available in figures 2.3 (a), (b), and (c). Experimental result for these dimension of L junctions are available in figures 2.3 (a), (b), and (c). Here analytical result is approximately similar to experimental on aspects, location and volume. With increase in inner fillet radius defect shifts towards centre and with increase in outer fillet radius defect decreases. No defect is present where radius of the fillet is equal to wall thickness as shown in figure 5.1c and proof is shown in figure 5.2. Figure 5.2 is zoomed view of centre of green region of figure 5.1c where bracketed term represents thermal gradient. Shrinkage volume is very small (order of 10-6 m3) compare to volume (approximately 0.09 m3) of L junction so that it can be neglected. Another problem occurs in L-junction is centerline weakness which may be present at the interface where two freezing fronts meet.

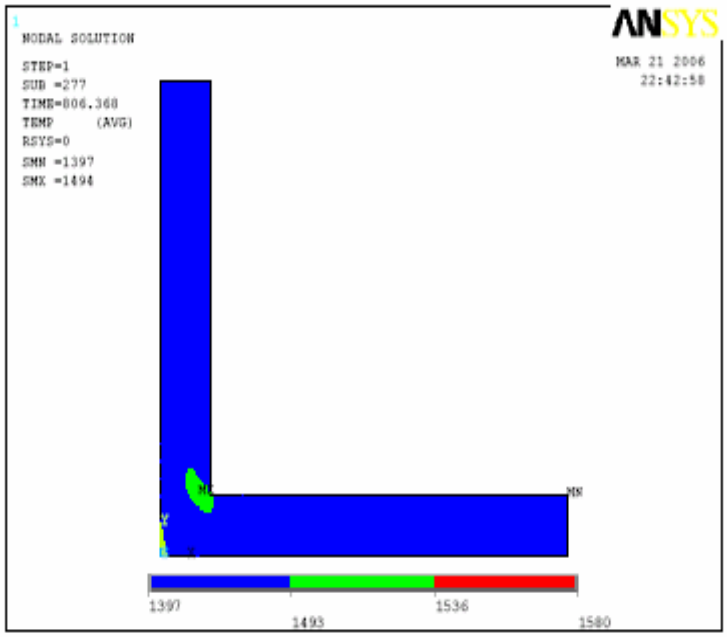

Figure 5.1a: L-junction without fillet

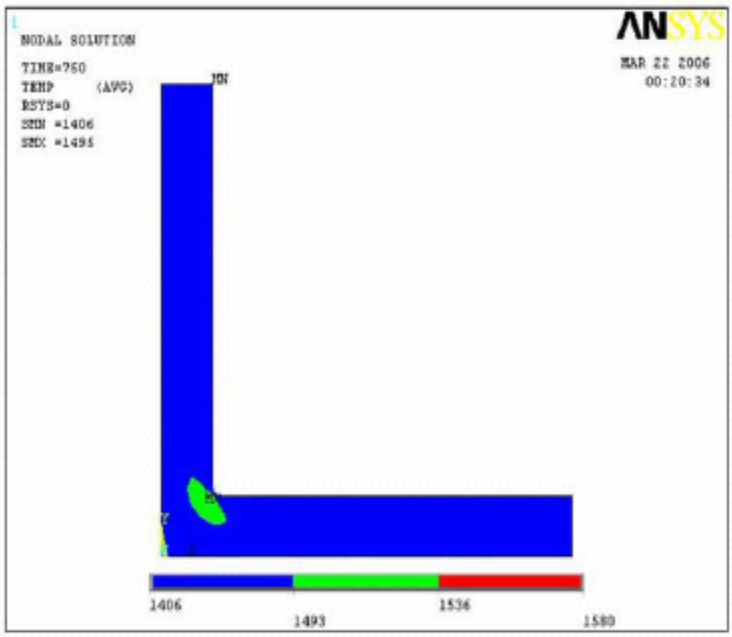

Figure 5.1b: L-junction with inner fillet radius .013 m

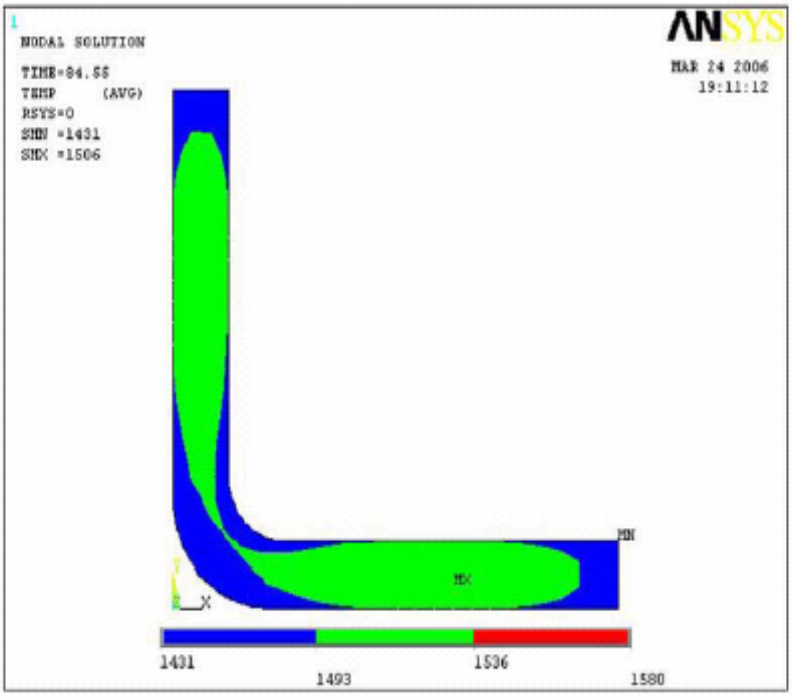

Figure 5.1c: L-junction with inner fillet radius 0.08 m and outer fillet radius 0.16 m

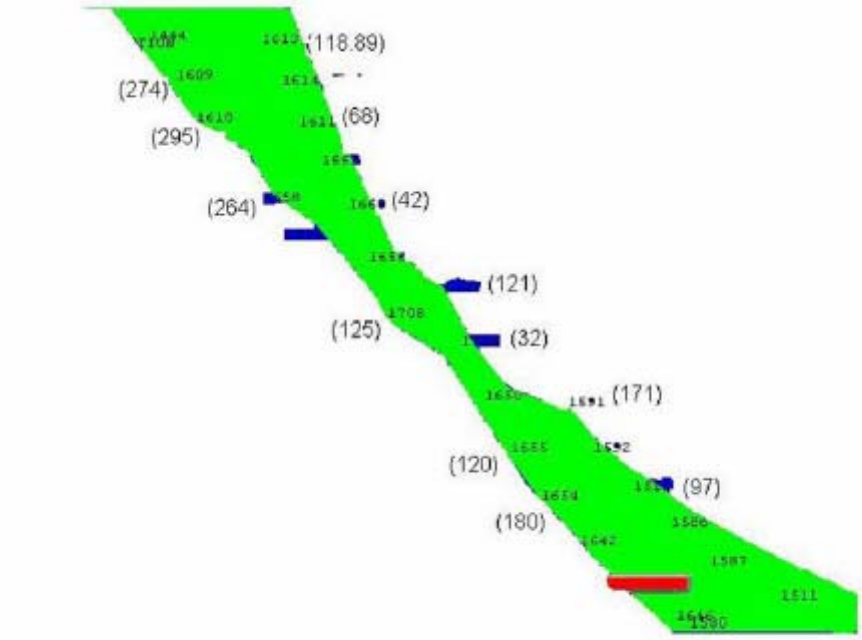

Figure 5.2: Zoomed view of figure 5.1c

5.3 V-Junction

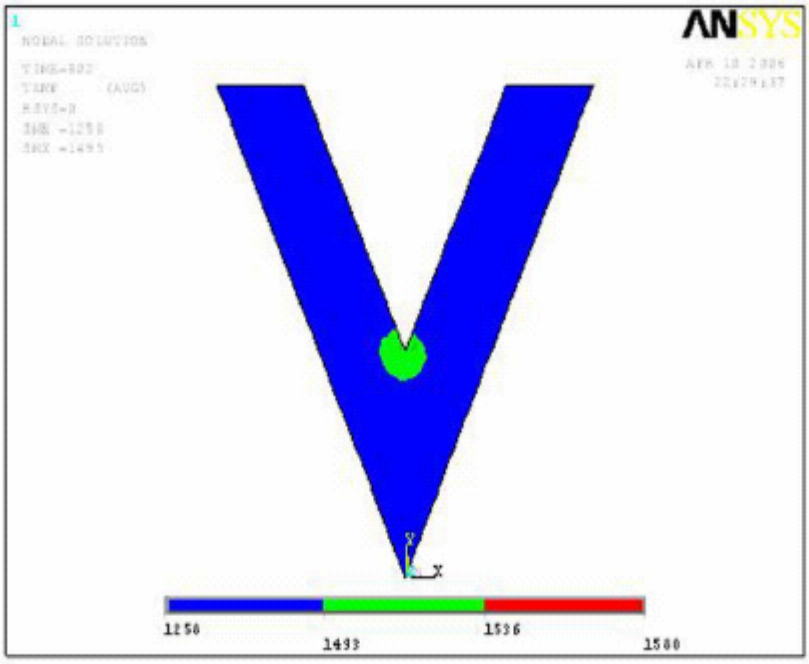

Figure 5.3a: V-junction without fillet

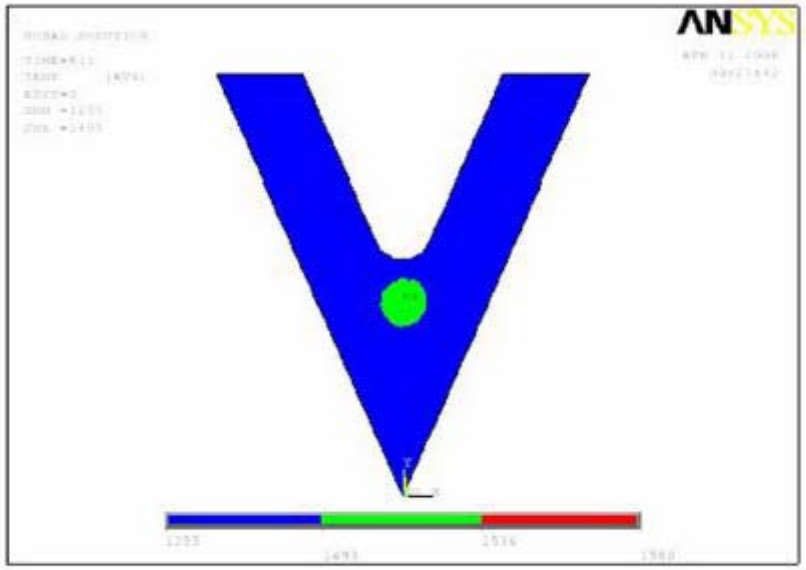

Figure 5.3b: V-junction with inner fillet radius 0.0254 m

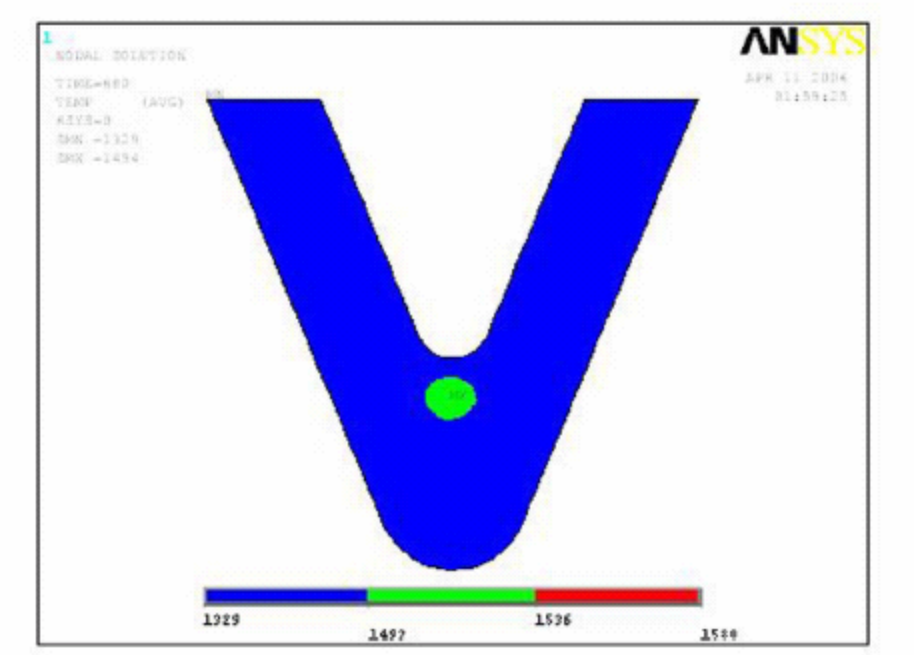

Figure 5.3c: V-junction with inner and outer fillet radius 0.0254 m and .0508 m

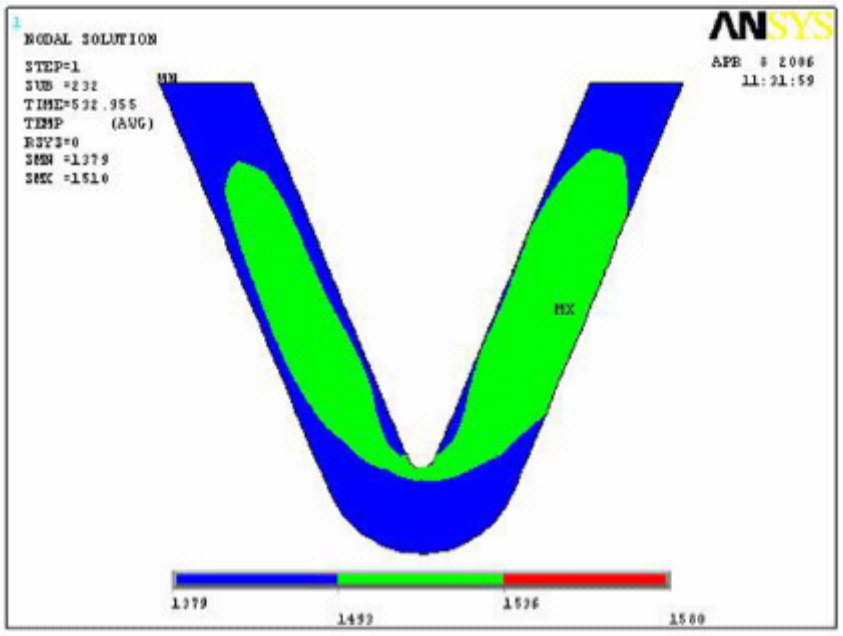

Figure 5.3d: V-junction with inner and outer fillet radius 0.0127 m and .0889 m

If it is formed by uniform sections then it will not be free from shrinkage cavities. In case of acute angle, shrinkage defect is much but with increase in angle shrinkage defect decreases due to increase in surface area. Effect of inner and outer fillet radius are same

as L-junction, means shrinkage defect increases with increase in inner fillet radius and decreases with increase in outer fillet radius. Defect can be reduced up to great extent by coring a hole or by decreasing wall thickness at the junction. Some examples of V-junction with defected volume are shown in figure 5.3. These belong to serial no 11, 12, 13 and 4 as listed in table 5.5. Shrinkage results are of same trend as per literature review and some examples are shown in figure2.3.

5.4 T-Junction

It is very difficult to get sound casting in case of T-junction. Shrinkage defect always increases with increase in fillet radius but smallest fillet compatible with other casting requirements are recommended. Shrinkage defect can be avoided by coring a hole but it affects on strength of T-junctions. Some examples of T-junction with defected volume are shown in figure 5.4. These belong to serial no 5, 7 and 12 as listed in table 5.7. Location of shrinkage defect is similar as shown in figure 2.3d,& e

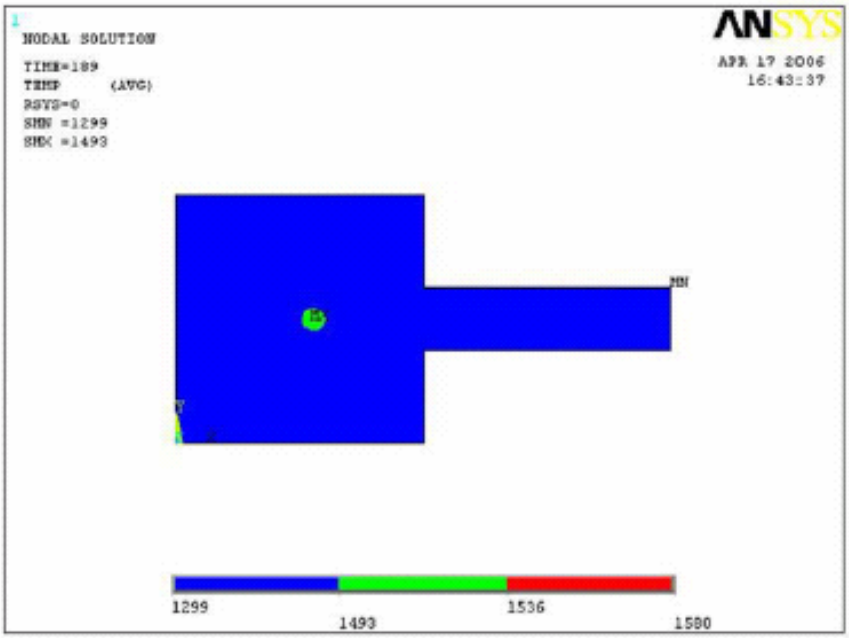

Figure 5.4a: T-junction without fillet

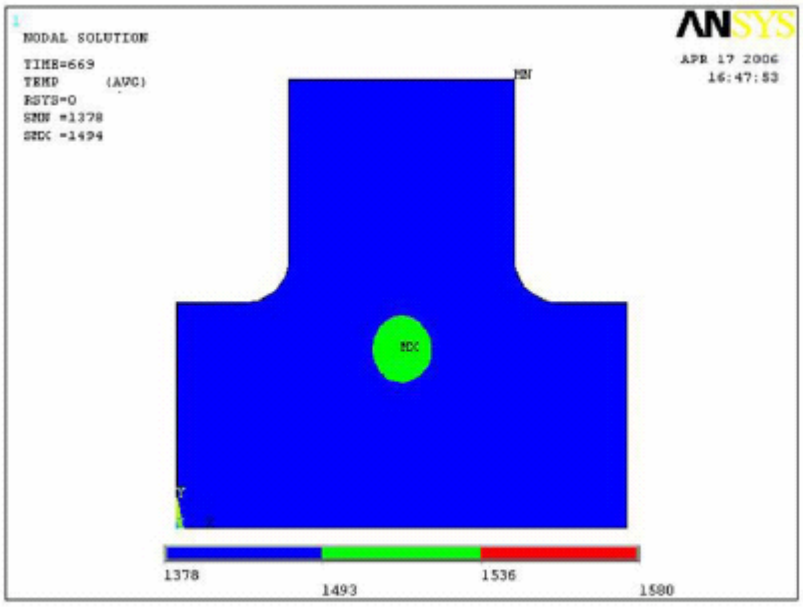

Figure 5.4b: T-junction with fillet radius 0.02 m

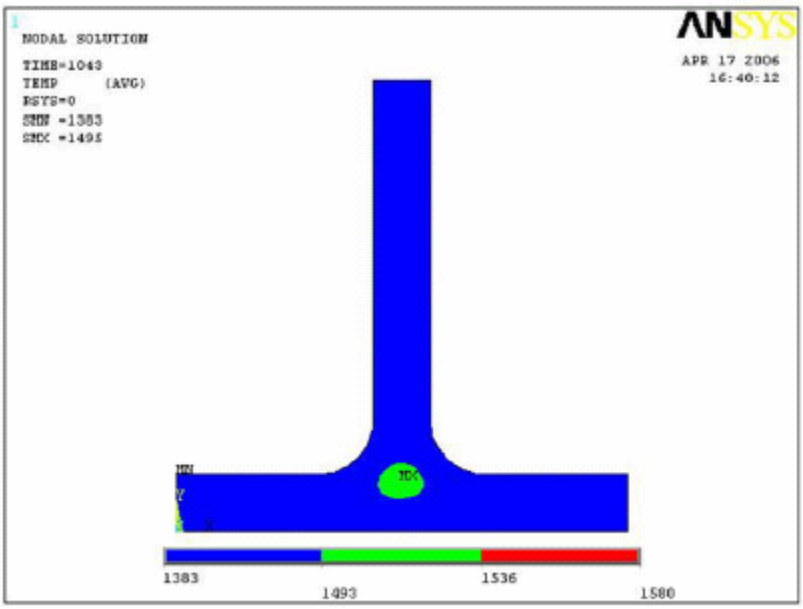

Figure 5.4c: T-junction with fillet radius 0.0762 m

5.5 X- Junction

Two examples of X-junctions are shown in figure 5.5 and experimental results are shown in figures 2.4 a, b. Experimental and analytical results are similar on both aspects location and shrinkage area. Shrinkage volume predicted by analysis is 0.36*10-2 m3 for figure

5.5a and 0.42*10-2 m3 for figure 5.5b, experimental result are 0.38*10-2 m3 and 0.4129*10-2 m3, both results are very close to each other. Fillet radius also increases shrinkage defect like other junctions. So that, by only one method shrinkage defect can be avoided and which is coring a hole.

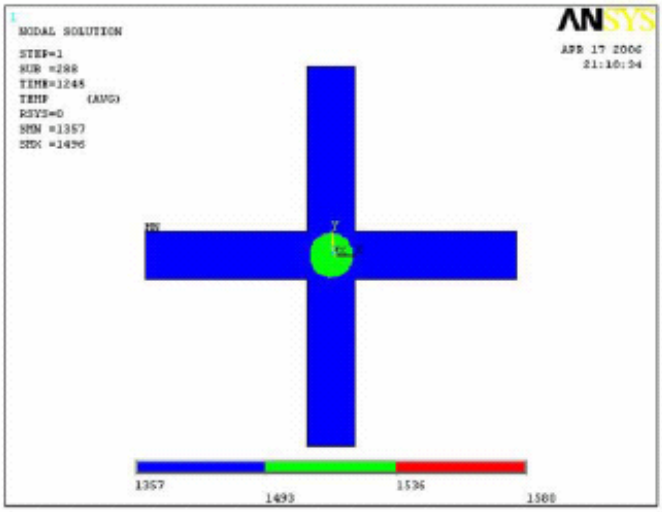

Figure 5.5a: X-junction without fillet

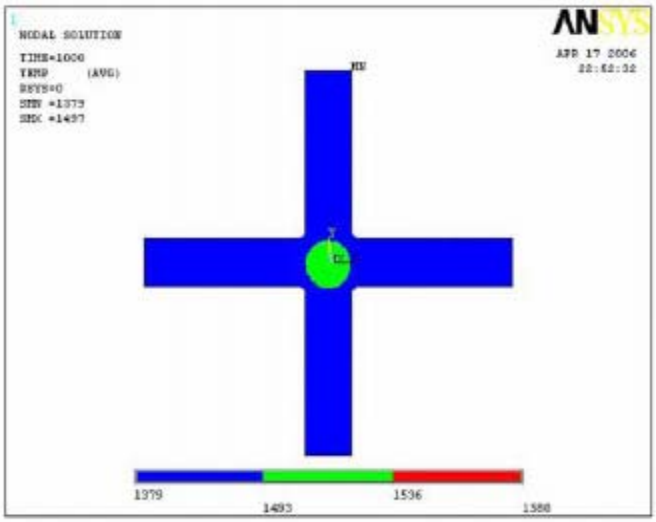

Figure 5.5b: X-junction with fillet radius 0.0127 m

5.6 LINEST Function and Regression Analysis of Junctions

It is well defined function in Microsoft Excel sheet and is used for regression analysis. It is based upon least squares method and calculates equation of straight line (in the form of equation 5.1) that best fits data.

$$y = m_1x_1 + m_2x_2 + m_3x_3 + m_4x_4 + \ldots\ldots\ldots\ldots + m_nx_n + b \qquad (5.1)$$

Where, the dependent y-value is a function of the independent x-values. The m-values are coefficients corresponding to each x-value, and b is a constant value. LINEST also returns additional regression statistics in tabular form as shown in table 5.1 and meaning of these terms are defined in table 5.2. The accuracy of the line calculated by LINEST depends on the degree of scatter in data. The more linear the data, the more accurate the LINEST model.

Table 5.1: Results of LINEST function

	A	B	C	D	E	F
1	m_n	m_{n-1}	……	m_2	m_1	b
2	se_n	se_{n-1}	……	se_2	se_1	se_b
3	r_2	se_y				
4	F	d_f				
5	SS_{reg}	SS_{resid}				

Table 5.2: Meaning of terms

Statistic	Description
$se_1, se_2, \ldots, se_n$	The standard error values for the coefficients $m_1, m_2, \ldots, m_n$.
se_b	The standard error value for the constant b.
r_2	The coefficient of determination, Compares estimated and actual y-values, and ranges in value from 0 to 1. If it is 1, there is a perfect correlation in the sample — there is no difference between the estimated y-value and the actual y-value. At the other extreme, if the coefficient of determination is 0, the regression equation is not helpful in predicting a y-value.
se_y	The standard error for the y estimate.
F	The F statistic or the F-observed value. F statistic is used to determine whether the observed relationship between the dependent and independent variables occurs by chance.
d_f	The degrees of freedom, is used to find F-critical values in statistical table and finally f-critical is used to find confidence level in model.
ss_{reg}	The regression sum of squares.
ss_{resid}	The residual sum of squares.

5.6.1 Regression analysis for L-junction

A typical L- junction is shown in figure 5.6, where A, B, R1, and R2 represent required dimensions to form L-junction. Results of shrinkage cavity predicted by thermal gradient method are shown in table 5.3 and are used for regression analysis. In table 5.3 last columns shows the experimental defected volume that is available in casting hand book and is very close to analytical result. LINEST function is used for regression analysis and result of function is shown in table 5.4. Serial number 8 and 16 are not used for regression analysis because there is no meaning of zero defect and regression results are also not good.

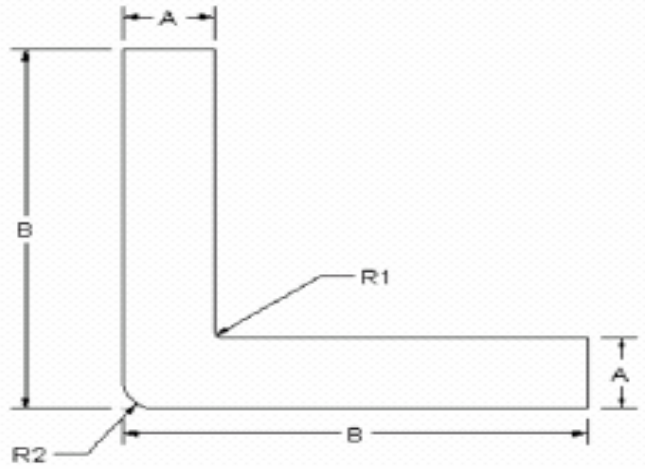

Figure 5.6: L-junction

Table 5.3: Shrinkage volume of L-junction for different combination of dimension

S. No.	A (m)	B (m)	R_2 (m)	R_1 (m)	Defect volume $*10^{-3}$ by analysis (m^3)	Defect volume $*10^{-3}$ by expt. (m^3)
1.	0.02	0.06	0	0	0.004017	……
2.	0.02	0.06	0	0.01	0.006265	……
3.	0.02	0.1	0	0	0.007066	……
4.	0.02	0.1	0	0.01	0.01652	……
5.	0.03	0.24	0	0	0.07822	……
6.	0.03	0.24	0.015	0.005	0.02441	……
7.	0.03	0.24	0	0.03	0.06176	……
8.	0.03	0.24	.05	0.03	0	……
9.	0.04	0.28	0	0	0.09138	……
10.	0.04	0.28	0.02	0.01	0.09462	……
11.	0.05	0.2	0	0	0.1288	……
12.	0.05	0.2	0	0.01	0.1672	……
13.	0.05	0.2	0.01	0.005	0.1239	……
14.	0.0762	0.6096	0	0	1.23	1.32
15.	0.0762	0.6096	0	0.0127	1.78	1.806
16.	.0762	06096	0.1524	0.0762	0	0
17.	0.0762	0.6096	0.0889	0.0127	0.35	0.387

Table 5.4: Result of LINEST function for L-junction

	A	B	C	D	E
1	1.772503	-11.69314	2.354357936	4.86021	-0.466488
2	7.832783	3.072889	0.835468047	7.452029	0.167351
3	0.85835	0.230041	#N/A	#N/A	#N/A
4	15.14917	10	#N/A	#N/A	#N/A
5	3.206704	0.529188	#N/A	#N/A	#N/A

So that, equation for L-junction is

$$S = (-0.47 + 4.86 * A + 2.35 * B + 1.77R_1 - 11.69R_2) * 10^{-3} \ \ m^3 \qquad (5.2)$$

Here S represents shrinkage volume. In table 5.4, coefficient of determination (r) is 0.85838 and is near to 1, so correlation is strong. Now, F-distribution is used here for other checkup. In table 5.4, F- statistic is 15.14 and F-critical is taken from book (Grewal, 1997). It depends upon three variables v1, v2 and α, where v1 is number of variables in the regression analysis, the term "Alpha" is used for the probability of erroneously concluding that there is a relationship and

$$v_2 = n - (v_1 + 1) \qquad (5.3)$$

Where n is number of data points. Here 05 . , 15 = = α *n* , 10 , 4 2 1 = = *v v* so that F-critical from the book is 3.48 and it is less then F-statistic so that it can be used for shrinkage prediction. Now by common sense, if there is increase in A, B, R1 then there is increase in shrinkage area, so it should be positive. Shrinkage area decreases with increase in R2, so it should be negative. In this case trend is same so that equation is acceptable. Results of shrinkage cavity predicted by critical solid fraction method are shown in table 5.5, and are used for regression analysis and result of regression analysis is shown in table 5.6.

Table 5.5: Shrinkage volume of L-junction for different combination of dimension

S. No.	A (m)	B (m)	R2 (m)	R1 (m)	Defect volume $*10^{-3}$ by analysis (m^3)	Defect volume $*10^{-3}$ by expt. (m^3)
1	0.05	0.2	0.05	0	0.09266	.....
2	0.076	0.6096	0.05	0	0.561	1.32
3	0.0762	0.6096	0	0.0127	1.049	1.806
4	0.0762	6096	0.17	0.0762	0.23	0
5	0.0762	0.6096	0.08	0.0127	0.3048	0.387
6	0.02	0.1	0	0.011	0.0061	.....
7	0.04	0.28	0	0	0.07286	.....
8	0.05	0.2	0.01	0.005	0.09702	.....
9	0.05	0.2	0	0.011	0.1027	.....
10	0.04	0.28	0.015	0.011	0.08	.....

Table 5.6: Result of LINEST function for L-junction

	A	B	C	D	E
1	5.244919	-5.80879	6.39E-06	18.25324	-0.612
2	12.42933	2.89918	0.000168	4.350127	0.221536
3	0.789762	0.197453	#N/A	#N/A	#N/A
4	4.695641	5	#N/A	#N/A	#N/A
5	0.732285	0.194937	#N/A	#N/A	#N/A

So that, equation for L-junction is

$$S = (-0.612 + 18.25 * A + 6.39 * 10^{-6} * B - 5.80879 * R_2 + 5.25 * R_1) * 10^{-3} \text{ m}^3 \qquad (5.4)$$

Here, S represents shrinkage volume. In table 5.6, r is 0.79, which is near 1 so that relation between dependent and independent variable is strong.

$v_1 = 5, v_2 = 7, \alpha = .05$

So that F critical is 4.53 and F-statistics (from table 5.6) is 4.69 and large compare to 4.53, means relation is perfect.

5.6.2 Regression analysis for V-junction

A typical V- junction is shown in figure 5.7 where, A, B, D, R1, and R2 represent dimensions of V-junction. Results of shrinkage cavity predicted by thermal gradient method are shown in table 5.7, and are used for regression analysis and result of regression analysis is shown in table 5.8. In table 5.7 last column represents the experimental defected volume which is available in casting hand book and is very close to analytical result.

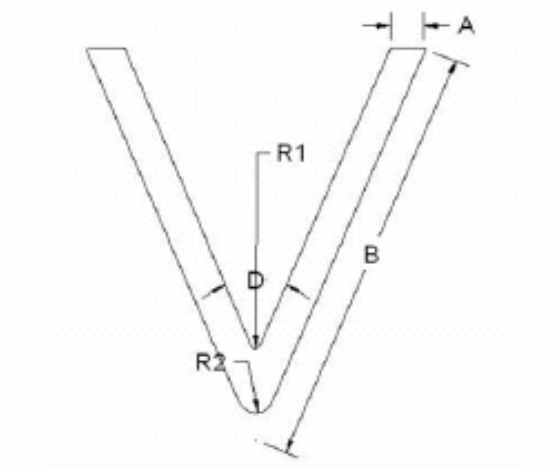

Figure 5.7: V-junction

So that by table 5.8,

$$S = (-1.39 + 30.48 * A + 39.83 * B - 5.14D + 52.65 * R_1 - 140.64 * R_2) * 10^{-4} \ \text{m}^3 \qquad (5.5)$$

Here, S is shrinkage volume. In table 5.8, r is 0.83, which is near 1 so that relation between dependent and independent variable is strong.

$v_1 = 5, v_2 = 7, \alpha = .05$

So that F- critical is 2.96 and F-statistics (from table 5.8) is 14.28 and large compare to 2.96, means relation is perfect.

By observation of figure 5.7, A, B and R1 are positive because with increase in these defect increases. Effect of D and R2 are reverse because with increase in D and R2 defect decreases, so both are negative. Trend of A, B, D, R1 and R2 are same in equation 5.5 as per expectation.

Table 5.7: Shrinkage volume of V-junction for different combination of dimension

S. No.	A (m)	B (m)	D (m)	R1 (m)	R2 (m)	Defected volume $*10^{-4}$ by ANSYS (m^3)	Defected volume $*10^{-4}$ by expt. (m^3)
1.	0.0825	0.6096	0.7854	0	0	26	21.29
2.	0.0825	0.6096	0.7854	0.0127	0	21.04	…….
3.	0.0825	0.6096	0.7854	0.0254	0	29.43	…….
4.	0.0825	0.6096	0.7854	0.0127	0.0889	12.03	7.62
5.	0.0825	0.6096	0.7854	0.0127	0.1016	4.749	…….
6.	0.0762	0.6096	1.047	0	0	23.04	…….
7.	0.0762	0.6096	1.047	0.0127	0.0381	9.82	…….
8.	0.0762	0.6096	1.047	0.0254	0	18.61	…….
9.	0.0762	0.32472	0.7854	0	0	6.282	…….
10.	0.0762	0.32472	0.7854	0.0254	0	8.018	…….
11.	0.0762	0.32472	0.7854	0.0254	0.0508	9.345	…….
12.	0.0762	0.43296	0.7854	0	0	11.2	…….
13.	0.0762	0.43296	0.7854	0.0254	0	13.98	…….
14.	0.0762	0.43	0.7854	0.0254	0.0508	7.304	…….
15.	0.0762	0.6	1.57	0	0	12.3	13.2
16.	0.0762	0.6	1.57	0	0.0127	17.8	18.06
17.	0.03	0.24	1.57	0	0	0.7822	…….
18.	0.03	0.24	1.57	0.015	0.005	0.2441	…….
19.	0.05	0.2	1.57	0	0	1.288	…….
20.	0.05	0.2	1.57	0	0.01	1.672	…….

Table 5.8: Result of LINEST function. For V-junction

S.N.	A	B	C	D	E	F
1	-140.638	52.65071	-5.13668	39.83188	30.48043	-1.39214
2	31.794	99.36754	4.804646	9.547542	129.7121	11.33064
3	0.836142	4.054505	#N/A	#N/A	#N/A	#N/A
4	14.28796	14	#N/A	#N/A	#N/A	#N/A
5	1174.4	230.1462	#N/A	#N/A	#N/A	#N/A

5.6.3 Regression analysis for T-junction

A typical T- junction is shown in figure 5.8 where, A, B, C, and R represent dimensions of T-junction. Results of shrinkage cavity predicted by thermal gradient method are shown in table 5.9, and are used for regression analysis and result of regression analysis is shown in table 5.10. In table 5.9 last column shows the experimental defected volume that is available in casting hand book and is very close to analytical result. LINEST function is used for regression analysis and result is shown in table 5.10.

Table 5.9: Shrinkage volume of T-junction for different combination of dimension

S. No.	A (m)	B (m)	C (m)	D (m)	R (m)	Defected volume $*10^{-4}$ by ANSYS (m^3)	Experimental volume $*10^{-3}$ (m^3)
1.	0.03	0.05	0.02	0.02	0	0.01439	.....
2.	0.081	0.081	0	0	0	0.3691	.....
3.	0.079	0.079	0.04	0.04	0	0.5322	.....
4.	0.079	0.081	0.04	0.04	0.01	0.3334	.....
5.	0.081	0.079	0.02	0.08	0	0.4398	.....
6.	0.079	0.079	0.02	0.08	0.01	0.3498	.....
7.	0.1	0.2	0.1	0.1	0.02	6.05	.....
8.	0.1	0.3	0.1	0.1	0	11.38	.....
9.	0.1	0.3	0.1	0.1	0.02	10.92	.....
10.	0.074	0.6	0.0762	0.53	0.0127	16.62	.....
11.	0.074	0.62	0.0762	0.53	0.0381	15.48	.....
12.	0.079	0.6	0.0762	0.533	0.0762	23	25.6
13.	0.0785	0.6	0.0762	0.5334	0	21	22.5
14.	0.074	0.62	0.0508	0.5334	0	11	.....
15.	0.0732	0.62	0.0508	0.5334	0.0127	14	12.2
16.	0.078	0.6	0.0508	0.5334	0.0254	19	.....
17.	0.074	0.62	0.0254	0.5334	0	13.6	.....

Table 5.10: Result of LINEST function. For T-junction

67.90593	0.058225	49.98895	24.94266	0.857178	-3.03613
41.76336	19.29234	37.22994	19.0711	57.89328	4.072621
0.920323	2.759374	#N/A	#N/A	#N/A	#N/A
25.41139	11	#N/A	#N/A	#N/A	#N/A
967.4298	83.75557	#N/A	#N/A	#N/A	#N/A

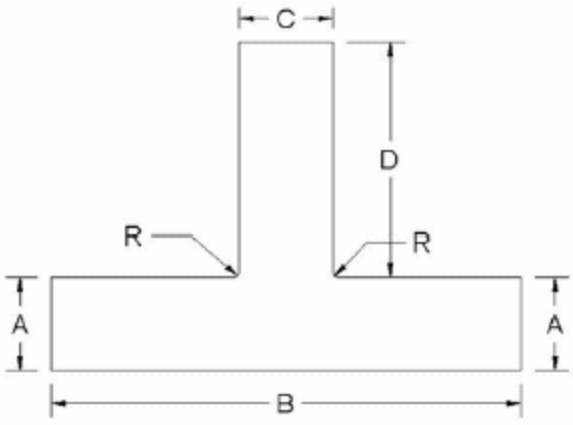

Figure 5.8: T-junction

So that, equation for T-junction is

$$S = (-3.04 + .86 * A + 24.94 * B + 49.99 * C + 0.058 * D + 67.91 * R) * 10^{-4} \ \text{m}^3 \qquad (5.6)$$

Here, S is shrinkage volume. In table 5.10, r is 0.92, which is near 1 so that relation between dependent and independent variable is strong.

$v_1 = 5, v_2 = 7, \alpha = .05$

So that Fcritical is 3.2 and F-statistics (from table 5.10) is 25.4 very large compare to 3.2, means By observation of figure 5.8, A, B, C, D and R are positive because with increase in these value defect increases. Trend of A, B, C, D, and R are same in equation 5.5 as per expectation. Results of shrinkage cavity predicted by critical solid fraction method are shown in table 5.11, and are used for regression analysis and result of regression analysis is shown in table 5.12.

Table 5.11: Shrinkage volume of T-junction for different combination of dimension

Sl. no.	A (m)	B (m)	C (m)	D (m)	R (m)	Defect volume $*10^{-4}$ by analysis (m^3)	Defect volume $*10^{-4}$ by expt. (m^3)
1.	0.08	0.08	0	0	0	0.21	…….
2.	0.08	0.08	0.04	0.04	0	0.28	…….
3.	0.08	0.08	0.04	0.04	0.01	0.34	…….
4.	0.08	0.08	0.02	0.08	0	0.35	…….
5.	0.1	0.3	0.1	0.1	0	11.2	…….
6.	0.0762	0.6096	0.0762	0.5334	0.0127	15.97	…….
7.	0.0762	0.6096	0.0762	0.5334	0.0381	15.34	…….
8.	0.0762	0.6096	0.0762	0.5334	0.0762	16.98	25.6
9.	0.0762	0.6096	0.0762	0.5334	0	12.9	22.5
10.	0.0762	0.6096	0.0508	0.5334	0	9.2	…….
11.	0.0762	0.6096	0.0508	0.5334	0.0127	8.1	12.2
12.	0.0762	0.6096	0.0508	0.5334	0.0254	12.63	…….
13.	0.0762	0.6096	0.0254	0.5334	0	16.34	…….

Table 5.12: Result of LINEST function For T-junction

	A	B	C	D	E	F
1.	57.34065	0.784149	3.863405	23.81747	273.5852	-23.7685
2.	47.22167	54.26023	56.6518	47.16774	462.9995	35.21668
3.	0.886802	2.963016	#N/A	#N/A	#N/A	#N/A
4.	10.96771	7	#N/A	#N/A	#N/A	#N/A
5.	481.4533	61.45626	#N/A	#N/A	#N/A	#N/A

So that, equation for T-junction is

$$S = (-23.77 + .27.58 * A + 23.82 * B + 3.86 * C + 0.78 * D + 57.34 * R) * 10^{-4} \ \text{m}^3 \qquad (5.7)$$

Here, S is shrinkage volume. In table 5.12, r is 0.88, which is near 1 so that relation between dependent and independent variable is strong.

$v_1 = 5, v_2 = 7, \alpha = .05$

So that Fcritical is 3.2 and F-statistics (from table 5.12) is 10.96 very large compare to 3.97, means relation is perfect.

5.7 Summary

• Junction is formed due to intersection of two or more casting sections. Shrinkage defect increases with increase in number of sections.

• In case of L and V junction, shrinkage defect increases with increase in inner fillet radius and decreases with increase in outer fillet radius, but fillet radius always increases shrinkage defect in T-junction and X-junction.

• Shrinkage defect decreases with increase in angle between two meeting sections.

Shrinkage defect can be reduced up to great extent by coring holes at junction but it affects strength.

• Equation 5.2, 5.4, 5.5, 5.6 and 5.7 can be used for shrinkage prediction of L, V and T junction.

Chapter 6

Conclusions and Future Work

6.1 Summary of Work Done

The main problem of junction solidification is shrinkage defect. This project focused on design guidelines for junction based on solidification analysis of L, V, T and X junctions.

1. There are mainly three methods for prediction of shrinkage defect and are based upon solid fraction ratio, thermal gradient and solidification rate.

2. Solid fraction method: When critical solid fraction ratio (fcr=0.67) loop disappears, it coincides with final generation portion of the shrinkage cavity in steel casting.

3. Gradient method: Shrinkage porosities in actual steel castings are found in those areas where the temperature gradient at the time of solidification is calculated to be **below 200 degree per meter.**

4. Material properties like thermal conductivity, density, and specific heat are varying with temperature which varies with time and makes the problem non-linear transient heat transfer. Finite element method is used to solve this non- linear problem.

5. In each and every case thermal gradient method is more accurate compare to solid fraction ratio.

6. In the field of junction design, shrinkage defects related to junction varies with parameters thickness, angle, and fillet. It can be avoided by proper size of fillet and coring hole.

7. Empirical equations for calculation of shrinkage volume (on the basis of thermal gradient and critical solid fraction ratio) for L, V, and T-junctions, which were discussed in chapter 5.

6.2 Limitations and Future Scope

The following are the few limitations of the work that has been done during the course of this project.

• The scope of project is limited for only ferrous metal because there is no available criterion to decide whether or not porosity will occur for other materials.

• This project has been done for L, V, T, and X- junction considering sand casting.

• No gating arrangement is considered in this project.

Further work can be done in the following areas of the project to increase the practical application of the project.

• Thermal analysis should be coupled with flow analysis for more accurate solution because shrinkage porosity formation involves heat flow and liquid metal flow.

• 3D analysis will give more accurate result compare to 2D analysis because heat flow is neglected in the perpendicular direction to the plane of section in case of 2D analysis.

• There is a need to simulate Y-junction to get shrinkage cavity for different dimension and finally for regression analysis.

• Formulation of single equation for all type of junctions with increase in number of variables.

• Implement the mathematical model in a computer program.

• Test the program on industrial casting.

References

1. American Society for Metals, "Casting Design Handbook", American Society for Metals, Ohio, pp. 49-56, 2002.

2. Chen, Y.H. and Im, Y.T., "Analysis of Solidification in Sand and Permanent Mold Castings and Shrinkage Predication", *International Journal of Machine Tools and Manufacture,* Vol. 30, No.2, pp. 175-189, 1990.

3. Chen, Y.M. and Wei, C.L., "Computer aided Feature based Design for Net Shape Manufacturing," *Computer Integrated Manufacturing Systems,* Vol.10, No. 2, pp. 147-164, 1997.

4. Dieter, G.E., "Engineering Design a Materials and Processing Approach," McGraw-Hill International Book Company, Boston, 1983.

5. Gao, Y.X., Yi, J.Z., Lee, P.D. and Lindley T.C., "A Micro-cell Model of the Effect of Microstructure and Defects on Fatigue Resistance in Cast Aluminum Alloys," *Acta Materialia,* Vol. 52, No. 19, pp. 5435-5449, 2004.

6. Grewal, B.S., "Higher Engineering Mathematics," Khanna Publishers, New Delhi, 35th Edition, 2000.

7. Gupta, O.P., "Finite and Boundary Element Methods in Engineering", Oxford & IBH Publishing Co. Pvt. Ltd, New Delhi, 1st Edition, 1999.

8. Gwyn, M.A., "Cost-Effective Casting Design: What Every Foundryman and Designer Should Know," *Modern Casting,* Vol. 88, No. 5, pp. 32-36, 1998.

9. Huan, Z. and Jordaan, G.D., "Galerkin Finite Element Analysis of Spin Casting Cooling Process," *Applied Thermal Engineering,* Vol. 24, No. 1, pp. 95-110, 2004.

10. Imafuku, I. and Chijiwa, K., "Application and Consideration of Shrinkage Cavity Prediction Method," *AFS Transactions,* Vol. 91, pp. 463-475, 1983.

11. Imafuku, I. and Chijiwa. K., "A Mathematical Model for Shrinkage Cavity Prediction in Steel Castings", *AFS Transactions,* Vol. 91, pp. 463-475, September/1983.

12. Niyama, I.E., Uchida, T., Morikawa, M. and Saito, M., "Predicting Shrinkage in Large Steel Castings from Temperature Gradient Calculation," *AFS International*

Cast Metals Journal, Vol. 6, No. 2, pp. 16-22, 1981.

13. Ravi, B., "Knowledge-based Casting Design," *Proc. of 62nd World Foundry Congress, Philadelphia, USA,* April 1998.

14. Ravi, B., "Metal Casting: Computer aided Design and Analysis," Prentice-Hall of India Pvt. Ltd., New Delhi, 1st Edition, 2005.

15. Robinson, D. and Palaninathan R., "Thermal Analysis of Piston Casting using 3D Finite Element Method," *Finite Elements in Analysis and Design,* Vol. 37, No.2, pp. 85-95, 2001.

16. Sachdeva, R.C., "Fundamentals of Engineering Heat and Mass transfer," New Age International (P) Limited, New Delhi, 2000.

17. Samonds, M., Morgan, K. and Lewis, R.W., "Finite Element Modelling of Solidification in Sand Castings Employing an Implicit-Explicit Algorithm," *Applied Mathematical Modelling,* Vol. 9, No. 3, pp. 170-174, 1985.

18. Venkatesan, A., Gopinath, V.M. and Rajadurai, A., "Simulation of Casting Solidification and its Grain Structure Prediction using FEM," *Journal of Material Processing Technology*, Vol. 168, No. 1, pp. 10-15, 2005.